Analysis of glacier hydrological model components with applications to Chile's Maipo Basin

Mumtaz Ahmad * and Mushfiqur Rahman

Posted Date: 28 June 2023

doi: 10.20944/preprints202306.1979.v1

Keywords: glacier hydrological modeling; mHM (Mesoscale Hydrological Model); degree day model

Article

Analysis of Glacier Hydrological Model Components with Applications to Chile's Maipo Basin

Mumtaz Ahmad [1] and Mushfiqur Rahman [2]

[1] Department of Environmental Science, Brandenburg University of Technology, 03046 Cottbus, Germany
[2] Institute of Water Modelling (IWM), Dhaka, Bangladesh
* Correspondence: mumtazahmad.btu@gmail.com; Tel.: (optional; include country code; if there are multiple corresponding authors, add author initials)

Abstract: During the dry season, glaciers contribute significantly to the water supply downstream, especially in areas with seasonal rainfall. It is important to have physical-based glacier models, which are more advanced in quantifying the future dynamics of glaciers and melt distribution. Toward this purpose, an investigation of different numerical modeling tools and their approach is conducted and planned further to incorporate a glacier module into a spatially distributed model called mHM (Mesoscale Hydrological Model, mhm-ufz.org). An open-source tool called MATILDA (Modeling Water Resources in Glacierized Catchments) is used beforehand to implement the glacier entities to the application catchment Maipo Basin in Chile. Due to limited time availability and source of data, the glacier melt of the MATILDA model is integrated into the mHM model to see what the implications would be if the glacier module was implemented from scratch in mHM. The analysis of the glacier hydrology resulting from the Maipo-Glacier model was carried out by comparing the modeled glacier flows with the total observed flows. To assess the credibility of the models, the results are compared based on three goodness-fit measures, specifically r^2Coefficient of Determination), NSE (Nash-Sutcliffe Efficiency), and KGE (Kling-Gupta Efficiency). Application of the mHM model in the Maipo basin in Central Chile is performed by using prepared input datasets, showing that the approach is viable as evidenced by a Kling-Gupta Efficiency of 0.80 and Nash-Sutcliffe Efficiency of 0.70 from the starting periods of 1950 to 2020. Overestimation by the mHM model occurs during the late summer season, particularly when temperature decreases. The MATILDA model is used on glacier melt distribution, forcing data is prepared from regional datasets, and a glacier profile is constructed from ice thickness datasets. According to the model, the average KGE result for the years 2012–14 and 2015–18 was respectively 0.44 and 0.41. Glacier melt produced by Matilda is in the range of 58-68 % of the total runoff and the glacier area decreased by 22-23% during the simulation period from 2012-14 and 2016-2018. A pilot sub-basin Olivares is used in the coupling mHM model with initializing MATILDA glacier melt. The new model is underestimated during the seasonal transition in the initial days of the simulation. A considerable portion of the ablation period might be missed because of the initial storage quality, true glacier extent, and height distribution being understated. In conclusion, the mHM model was capable of predicting runoff well in a mountainous region and could also serve as a monitoring tool for watershed management. There are differences in results between the two models because of the different spatial resolutions and methodologies. MATILDA have a glacier retreat routine that gives better result for the glacier characteristics such as. A new glacier dynamics model needs to be implemented in the future to develop intermediate complexity, bridge catchment, and glacier scales after using the mHM, MATILDA, and mHM with MATIDLA model for analysis of glacier and highlighting the model's deficiencies in the initial period of simulative assessments.

Keywords: glacier hydrological modeling; mHM (Mesoscale Hydrological Model); degree day model

1. Introduction

There are approximately 2 billion people around the world whose water supply is dependent on glacial meltwater [1]. A glacier can provide a vital multiannual buffer as a valuable natural water reservoir, especially in drought-prone regions [2, 3]. In many parts of the world, large rivers originate

from mountain areas where snow and glaciers store a large quantity of fresh water. A total of 75% of the world's freshwater is stored in glaciers, 99.5% of which is found in Antarctica and Greenland (IPCC, 1996). Their influence can be seen in several important areas such as flood control, sediment transport, irrigation, water consumption, and hydroelectric generation because they control the hydrological regime in mountainous areas. There are different time scales on which glaciers play the role of water stores and regulators of the hydrological regime, short-term processes e.g. flood on a daily or sub-daily basis, medium-term processes, seasonal and inter-annual fluctuations in hydrological regimes in glaciated areas, and long-term processes changes in sea level [4].

In the past decade, glaciers in most parts of the world have been retreating, resulting in a wide range of implications, from global effects on sea levels and ocean systems to regional [5] and local effects on catchment hydrology [6]. Glaciers have been retreating strongly [7] and are expected to continue doing so throughout the 21st century [8], their role in the water cycle will change. It appears that 'peak water has already passed in many basins around the world, indicating a recent change from glacial to naval-pluvial regimes' [9]. In addition to impacting millions of people's water supply, this could also increase the likelihood of natural hazards, increase hydro-political tensions [10], and undermine the reliability of many ecosystems impacted by glacial meltwaters [11]. The change in glacier runoff due to glacier retreat is a concern, especially in areas where glacier runoff is an important source of water for agriculture, industry, and municipalities. It is therefore essential to investigate the hydrology of glaciers at these watersheds. Demographic pressure, changing climate, and glaciers' shrinking under climate change pose a serious threat to water security in the Andean region [12]. Recent studies have demonstrated glacier retreat and thinning in central Chile over the twentieth century, with an average estimate of 12.8% of glacier area loss over the 51 years between 1945 and 1996 [13]. With over 7 million inhabitants, the Santiago region uses 70 to 90 percent of its agricultural water from the Maipo River [14]. Meltwater is essential for both agriculture and urban centers of growing demographic and economic importance during the summer. Competition for water allocation grows as water use increases as the population increases and the country becomes more industrialized [15, 16, 17]. Pellicciotti et al. [18] reviewed the recent status of Chilean glaciers and found that the central Andes glaciers, specifically Juncal Norte, Juncal Sur, and Olivares Gamma glaciers, which are in the Maipo catchment, have been shrinking rapidly since 1955. Their area has been declining by 2.4%, 10.9%, and 8.2%, respectively. Over the next century, water use is expected to rise [19] on the other hand temperature trends at locations throughout the region [20], including the upper river basin, show that summer and winter air temperatures have increased statistically significantly since the 1970s [21]. An increase in air temperature is likely to influence the summer snowmelt phase, by enhancing it, and the winter precipitation phase, by reducing the amount of snow accumulated at the start of the melt season [22].

It has been shown by Carrasco et al. [20] that the snow line in central Chile has risen by 127 measures over the last quarter of the twentieth century. There has been great progress in glacier modeling encyclopedically in the once many times [23]. Indeed, however all these approaches produce harmonious results at the global position, their indigenous and original results are subject to lesser misgivings [24]. Several reasons contribute to this, similar to the high position of abstraction of the key processes, the need to spatially fit the model parameters, and the query in the boundary and initial conditions [24, 25]. The maturity of models doesn't include ice dynamics, has no anterior ablation [26], and warrant modulation of the mass balance face by debris cover and snow redivision (winds and avalanches). Among the available models, only one [24] was suitable to give estimates of once glacier volume changes and there's no open-source interpretation of these models.

The use of a spatial glacier model is pivotal to constructing a model for assaying changes in glacier mass over time. To negotiate this, automatic initialization styles are needed, and several different approaches have been used in the development of hydrological models to integrate the snow and ice melting processes [27, 28]. Among the models, Snowmelt Runoff Model (SRM) and the HBV model are extensively used to study the effects of climate change on glaciers grounded on meteorological data, satellite data about snow cover, and climate scripts [29, 30, 31].

 doi:10.20944/preprints202306.1979.v1

In this paper, we probe how including glaciers in a hydrologic model impacts its performance and enhances the being models. The original idea was to develop a completely distributed physically grounded glacier hydrological model able to develop the mass balance process. Accordingly, a glacio-hydrological model tool is planned to develop as an extension to the being mHM (The Mesoscale Hydrologic Model) with post-processing and visualizations. The hydrological model (mHM) is developed in the Fortran programming language and due to time and resource constraints, the original idea was changed from developing the glacier module into mHM to assaying glacier hydrological models and understanding the counteraccusations of the glacier model being implemented into mHM.

It's within the environment of taking robust representations of glaciers in hydrological models since glacier melt is an important contributor to sluice inflow. This thesis seeks to contribute to the understanding of how dependable models that have minimum data demands, similar to MATILDA (Modeling Water coffers in Glacierized Catchments), can be applied successfully in different catchments and how the full query of their catchment runoff protrusions can be reckoned for and understood.

This thesis explores how including glaciers in a hydrologic model impacts the model's performance and enhances existing hydrologic models. An open-source tool called MATILDA (Modeling Water Resources in Glacierized Catchments) is used to analyze the glacier catchment and compare it with a hydrological tool mHM using grid cells as the primary hydrologic unit and is spatially explicitly distributed. The purpose of this analysis is to gain insight into the differences between running a snow melt module and a glacier melt module. As case studies, the evolution of the glacier in the entire mountainous area of the Maipo basin in Santiago, Chile is investigated using regional climate scenarios.

The initial objective of the thesis is divided into different targets. Firstly, mHM is performed for the whole Maipo basin as per the workflow described in Figure 7 and then MATILDA (Modeling Water Resources in Glacierized Catchments) is performed for the whole Maipo basin. To integrate MATILDA melt into mHM, a pilot sub-basin is performed with the MATILDA model, and then the output melt is incorporated into the mHM model as per the workflow described in Figure 9 and then the mHM model runs again with the MATILDA melt.

2. Materials and Methods

The study areas for this research consist of the catchment area of the Maipo River Basin Rio Maipo En El Manzano catchment as shown in Figure 1, with the gauge id "5710001" located in Central Chile close to a small town El Manzano along the river, about 15 km upstream of Santiago. The basin is located between the latitudes 32.92° to 34.29° and, longitude 69.77° to 71.63°, with an area of approximately 4839.04 km^2 and altitude, varied between 890 m a.s.l to more than 6500 m a.s.l. Around only 10% of the area is below the 2000 and 40% is below the 3000 m a.s.l. The average flow at the El Manzano gauge station was 120 m^3/s from 1980–2013 and it is a fundamental natural resource for cities, including the Chilean capital Santiago, whose population comprises 40% (~7 million) of the country.

The Maipo River Basin contains high mountain basin areas and a total of 364 km^2 of the area was covered by glaciers, which accounted for approximately 8% of the area. (1980–2013). According to the Chilean glacier inventory, approximately 1000 individual ice bodies could be found in this region, including ice bodies with debris-free or debris-covered surfaces, and rock glaciers. This represents approximately 1.7% of the total area of Chile covered by glaciers. Glacier surfaces range from 21 km^2 (Juncal Sur Glacier) to 0.01 km^2. The mountain area of the Maipo basin is further divided into 5 sub-basins to investigate glacier modeling. The Upper Maipo basin has the highest basin area and lowest maximum elevation compared to other basins. The Colorado Basin has the maximum elevation of the glacier.

Preprints (www.preprints.org) | NOT PEER-REVIEWED | Posted: 28 June 2023 doi:10.20944/preprints202306.1979.v1

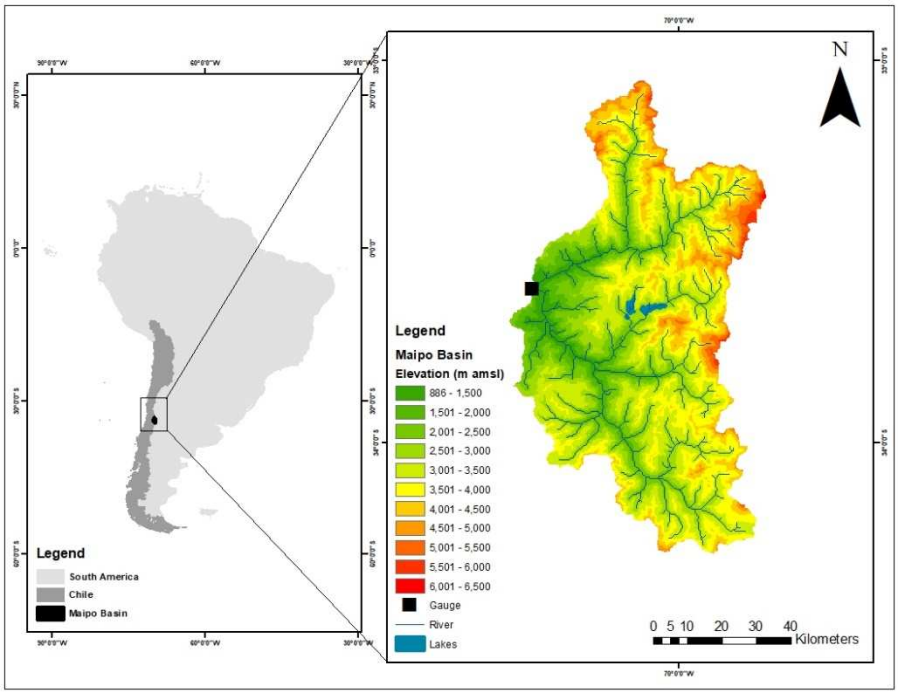

Figure 1. A case study in Maipo Basin and the location of gauge, river, and lakes.

2.1. Meteorological Data Preprocessing.

The meteorological data used in this application is obtained from the ERA5 [32] and CAMELS-CL database, for the basin Rio Maipo En El Manzano (5710001) where the station is installed. The CAMELS-CL website provides information from S16 fluviometric stations throughout Chile, including daily flow data as well as daily meteorological data. The meteorological data were obtained from the ERA5 dataset with a resolution of 27-28km, and the observed discharge was obtained from the gauge station located at CAMLES Cl from 2011-2018. According to Table 1, data from 2011-2018, the average discharge was 77.41 $\mathbf{m^3/s}$, so it has decreased when compared to 1980-2015. In autumn 2016, the maximum discharge was recorded at 526 $\mathbf{m^3/s}$, which is unrealistic considering the precipitation during that period shown in Figure 2, so it may have been due to radiation or sunshine, or even an outburst of catchment storage.

Table 1. Daily Meteorological Metadata from 2011-2018.

	Dis(m^3/s)	Preci(mm)	Temp(C°)	PET(mm)
Mean	77.41	2.97	2.70	2.04
Min	26.3	0	-16.51	0.06
Max	526	104.30	16.58	5.43
Std	39.97	7.47	6.21	1.27

The mean precipitation is recorded as almost 3 mm from 2011 to 2018 with a maximum of 104.3 mm. Over the period 2011 to 2018, maximum and minimum temperatures ranged from -16 to +16 C°, with an average of 2.7 C°. A mean evapotranspiration of 2.04 mm was recorded between 2011 and 2018, with a maximum of 5.43 mm.

According to Figure 2, discharge showed two peaks during the Autumn of 2012 and 2016, for the first peak precipitation is also showing a high rise during that time, and the second peak didn't show a strong rise from the precipitation. There is a maximum rise in precipitation during the middle of 2015, which exceeds 100 mm. A phase transition occurs in both temperature and evapotranspiration during the change of seasons. The summer season (January) recorded maximum, whereas the winter season contains low temperatures and evapotranspiration.

Preprints (www.preprints.org) | NOT PEER-REVIEWED | Posted: 28 June 2023 doi:10.20944/preprints202306.1979.v1

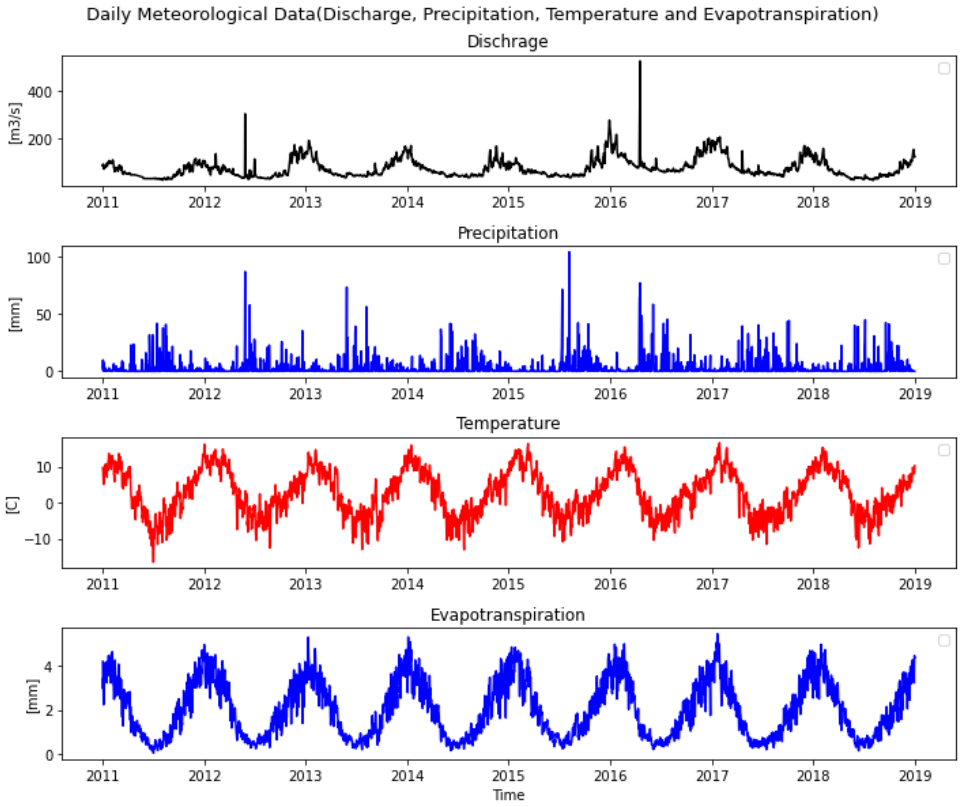

Figure 2. Daily Meteorological Data (Discharge, Precipitation, Temperature, and Evapo.).

Table 2 shows the correlation between discharge, temperature, precipitation, and evapotranspiration. Discharge has the best correlation with evapotranspiration and a negative correlation with temperature. The temperature has a negative correlation with all three parameters. Precipitation has the best correlation with evapotranspiration which is also shown in Figure 3.

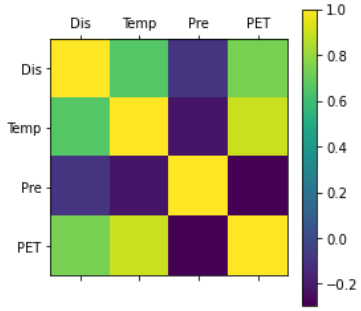

Figure 3. Correlation Matrix.

Table 2. Daily Meteorological data correlation.

	Dis	Temp	Pre	PET
Dis	1.0	-0.09	0.65	0.73
Pre	0.65	-0.22	1.0	0.89
Temp	-0.09	1.0	-0.22	-0.29
PET	0.73	-0.29	0.89	1.0

2.2. Morphological Data Preprocessing

A vector and raster version of the Maipo basin is used to perform geospatial analysis and a data description is given in Table 3. Hydro-basin of the Maipo catchment has been extracted from the gridded HydroSHEDS (Hydrosheds.org) as a vectorized polygon. For extracting elevation masks of

Preprints (www.preprints.org) | NOT PEER-REVIEWED | Posted: 28 June 2023 doi:10.20944/preprints202306.1979.v1

the basin SRTM-DEMs raster data is used which is created using bi-static radar interferometry with a resolution of 30m. SRTM is created on a near-global scale between 56°S and 60°N, using C-band and X-band radar frequencies by the National Aeronautics and Space Administration (NASA), and German Aerospace Center (DLR).

Table 3. Spatial Data Sets Used for Setting Up the mHM Model and MATILDA.

Sort	Format	Description	Resolution	Source
DEM	Raster	SRTM	30m	Tachikawa et al., 2011
Basin	Vector	HydroBasin	Polygon	Lehner, B., Grill G. (2013)
Glacier Outlines	Vector	Glacier Outlines RGI v6.0	Polygon	Pfeffer et al., 2014
Glacier Profile	Raster	Glacier Ice thickness	25m	Farinotti D., M. Huss 2019

The glacier outlines are taken from the Randolph Glacier Inventory (RGIv6) [33], with the position being Chilean glaciers, between-18 and-56 degrees, and latitude at release date 2018-07-24. In the Maipo River Basin, the non-gap filled DEM shows a veritably good content, except for many small glaciers, which weren't included (e.g., Morado Glacier) face hypsometry for each glacier is deduced from cutting the outlines with Digital Elevation Models (DEMs). Ice consistency distribution of all glaciers of the Maipo basin is downloaded from the ETH Zurich exploration collection website and a Civilians routine is followed to achieve the hypsometry of the glacier.

Figure 4 represents the Maipo receptacle with its sub-basin, which is created for concentrating individual sub-basin to compare the glacier model for better output results. Figure showing the elevation of the glacier with elevation from 2500m to 6500 m amsl (above mean ocean level) and ice consistency with maximum 355m.

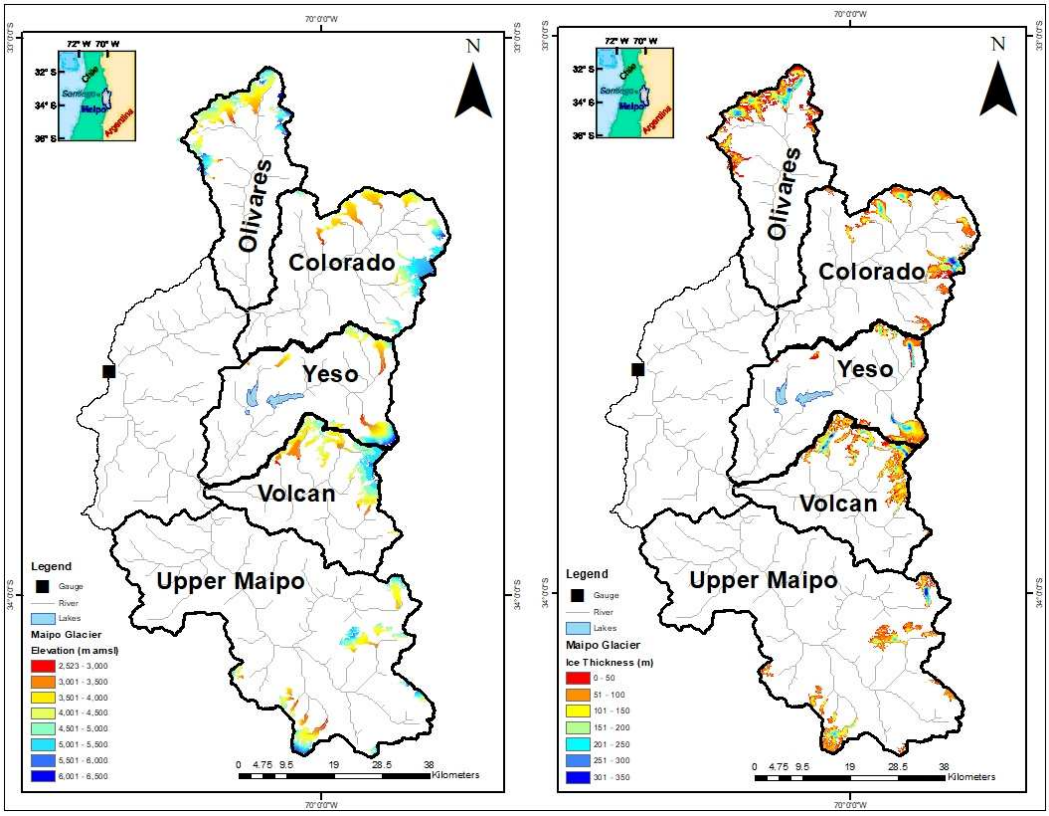

Figure 4. Maipo Sub-Basin Glacier Elevation and Ice Thickness.

An overview of the different Maipo basins is outlined in Table 5. Olivares basin has 12 glaciers consisting of 79.99 km^2 of area, 5925m maximum elevation, 3422 m mean elevation, and with max

Preprints (www.preprints.org) | NOT PEER-REVIEWED | Posted: 28 June 2023 doi:10.20944/preprints202306.1979.v1

326.84m ice thickness. The Colorado basin has 16 glaciers covering a 67.07 km^2 area, 6334 m of maximum elevation, and 2955 m mean elevation. The ice thickness is 293.70 m in the Colorado basin glaciers. Yeso basin has only 6 glaciers covering 67.05 km^2 which means the Yeso basin has the maximum area ratio as compared to other basin glaciers.

The maximum and mean elevation is 5904 m, and 3567 m, and the ice thickness is 219.04 m of the Yeso basin. The Volcan basin has 13 glaciers consisting of 70.62 km^2 of area, which is the second most glacierized area in the Maipo basin after the Olivares basin. The maximum and mean elevation is 5676 m, and 3367 m and ice thickness is 245.67m of Volcan basin. The Upper Maipo basin has 18 glaciers covering 59.22 km^2 of the area and maximum, mean elevation of 5404 m, 3319 m, and ice thickness of 271.17 m.

Table 4. Characteristics of Maipo Sub-basin .

Basin Name	Lan & Lon	Area (km^2)	Mean Elev(m)	Max Elev(m)	No. of Glaciers	Glacier Area (km^2)	Max. Ice Thickness
Olivares	-33.49,-70.14	541.6	3690	6049	12	79.99	326.84 m
Colorado	-33.49,-70.13	783.4	3737	6550	16	67.07	293.70 m
Yeso	-33.80,-70.21	626.6	3567	5904	6	67.05	219.04 m
Volcan	-33.81,-70.21	523.4	3367	5676	19	70.62	245.67 m
Upp. Maipo	-33.98,-70.15	1035.5	3319	5404	18	59.22	271.17 m

2.3. mHM (mesoscale hydrological model)

The mesoscale Hydrologic Model (mHM, https://mhm-ufz.org) is a spatially explicit, grid-based hydrologic model. It is designed specifically to provide distributed predictions of various hydrologic variables such as runoff, evapotranspiration, soil moisture, and discharge along rivers. The model simulates the following processes: canopy interception, snow accumulation and melting, soil moisture dynamics, infiltration, surface runoff, evapotranspiration, subsurface storage, and discharge generation, deep percolation and baseflow, discharge attenuation, and flood routing.

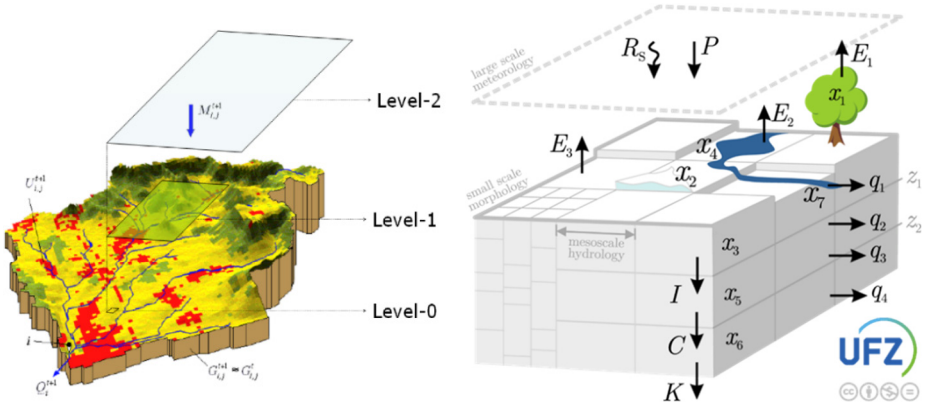

Figure 5. Hierarchy of data and modeling levels in mHM (https://mhm-ufz.org) & mHM cell [34].

A mesoscale view of the hydrological cycle spans several orders of magnitude and consists of three levels (mHM levels), differencing them to better capture the spatial variability of variables and states.

- Level-0: Spatial discretization suitable for representing the main terrain features, various soil characteristics (photos), the land cover, and the cell sizes is denoted by L0.
- Level-1: Spatial discretization is used to describe dominant hydrological processes at the mesoscale and geological formations of the basin. This level's cell size is denoted by L1.
- Level-2: Spatial discretization suitable to describe the variability of the meteorological forcing at the mesoscale, for example, the formation of convective precipitation. The cell size at this level is denoted by L2.

Preprints (www.preprints.org) | NOT PEER-REVIEWED | Posted: 28 June 2023 doi:10.20944/preprints202306.1979.v1

A mesoscale basin is a natural system composed of very heterogeneous materials with fuzzy boundary conditions. It is quite difficult to justify the continuity assumption of the input variables because most of the spatial heterogeneity of a basin can be explained by discrete attributes, such as soil texture, land cover, and geological formations. Therefore, a system of ordinary differential equations ODEs [35] was adopted to describe the evolution of state variables at a given cell i within the domain Ω. This system of ODE:

$$\dot{x}_{1i} = P_i(t) - F_i(t) - E_{1i}(t)$$
$$\dot{x}_{2i} = S_i(t) - M_i(t)$$
$$\dot{x}_{3i}^{l} = (1-\rho^{l})I_i^{l-1}(t) - E_{3i}^{l}(t) - I_i^{l}(t)$$
$$\dot{x}_{4i} = \rho^{1}(R_i(t) + M_i(t)) - E_{2i}(t) - q_{1i}(t)$$
$$\dot{x}_{5i} = I_i^{L}(t) - q_{2i}(t) - q_{3i}(t) - C_i(t)$$
$$\dot{x}_{6i} = C_i(t) - q_{4i}(t)$$
$$\dot{x}_{7i} = \hat{Q}_i^{0}(t) - \hat{Q}_i^{1}(t) \qquad Eq: 1-7$$
$$\forall i\ \Omega\ \epsilon A$$

Where,

Table 5. Equations 1-7 parameters with description.

States	Description
x_1	Depth of the canopy storage, mm
x_2	Depth of the snowpack, mm
x_3	Depth of soil moisture content in the root zone, mm
x_4	Depth of impounded water in reservoirs, water bodies, or sealed areas, mm
x_5	Depth of the water storage in the subsurface reservoir, mm
x_6	Depth of the water storage in the groundwater reservoir, mm
x_7	Depth of the water storage in the channel reservoir, mm

Inputs	Description
P	Daily precipitation depth, mm d^{-1}
T	Daily mean air temperature, °C
E_p	Daily potential evapotranspiration (PET), mm d^{-1}

Outputs	Description
$\hat{Q}_i^0$	Simulated discharge entering the river stretch at cell $i, m^3\ s^{-1}$
$\hat{Q}_i^1$	Simulated discharge leaving the river stretch at cell $i, m^3\ s^{-1}$

Preprints (www.preprints.org) | NOT PEER-REVIEWED | Posted: 28 June 2023 doi:10.20944/preprints202306.1979.v1

Fluxes	Description
S	Snow precipitation depth, mm d^{-1}
R	Rain precipitation depth, mm d^{-1}
M	Melting snow depth, mm d^{-1}
E_p	Potential evapotranspiration, mm d^{-1}
F	Throughfall, mm d^{-1}
E_1	Actual evaporation intensity from the canopy, mm d^{-1}
E_2	Actual evapotranspiration intensity, mm d^{-1}
E_3	Actual evaporation from free-water bodies, mm d^{-1}
I	Recharge
C	Percolation, mm d^{-1}
q_1	Surface runoff from impervious areas, mm d^{-1}
q_2	Fast interflow, mm d^{-1}
q_3	Slow interflow, mm d^{-1}
q_4	Baseflow, mm d^{-1}

Indices	Description
l	Index denoting a root zone horizon, /=1, L (say L= 3), in the first layer, $0 \leq z \leq z_1$
t	Time index for each Δr interval
ρ^l	Overall influx fraction accounting for the impervious cover within a cell

To run mHM, we need several datasets such as meteorological, morphological variables, land cover, and gauging station information. All the meteorological variables are downloaded in NetCDF format and have hard-coded names such as 'tavg' for average temperature, 'pre' for precipitation, and 'pet' for evapotranspiration. There is an additional file called header.txt in every meteorological data file, and the easting and northing coordinates of the lower left corner should correspond to your catchment's morphological data. To maintain consistency in data, NODATA (-9999) value is specified in the header file. In addition, input mHM needs a latlon.nc file that specifies every grid cell's geographical location in WGS84 coordinates. The input for mHM also requires a latlon.nc file specifying the geographical location of each grid cell in WGS84 coordinates. Each resolution of the hydrological simulation at level-1 has to be adjusted. There are several morphological input datasets needed for MHM, and all of them must be provided in ArcGIS ASCII format, which stores the above header data and the actual data as plain text. Some raster files need to be supplemented with look-up tables that provide additional information. The required datasets and their corresponding filenames are given in Table 8:

Preprints (www.preprints.org) | NOT PEER-REVIEWED | Posted: 28 June 2023 doi:10.20944/preprints202306.1979.v1

Table 8. Morphological data for mHM initialization.

Description	Raster, File name
Sink filled Digital Elevation Model	dem.asc
Slope map	slope.asc
Aspect Map	aspect.asc
Flow Direction map	fdir.asc
Flow Accumulation	facc.asc
Gauge(s) position	idgauges.asc, .txt
Soil map	soil_class.asc, .txt
Hydrogeological	geology_class.asc, .txt
Leaf Area Index	LAI_class.asc, .txt
Land use map	lc.asc

Figure 6 illustrates the workflow of the mHM model, a mHM setup is developed in Fortran 90 language and Linux system is used to run the model. Maipo basin including the meteorological forcing files and morphological files are prepared by UFZ Leipzig and used in this study. An mHM compilation file is required to run the mHM model for new applications and mhm.nml(namelist file) from the default model is used. After setting all the parameters for the Maipo basin and changing the name of the file as per Table 8, the model is run as daily output. For post-processing the output result, python is used for plotting and visualization. All the mHM model files including input and output results available and shown in Table 21 Digital Appendix.

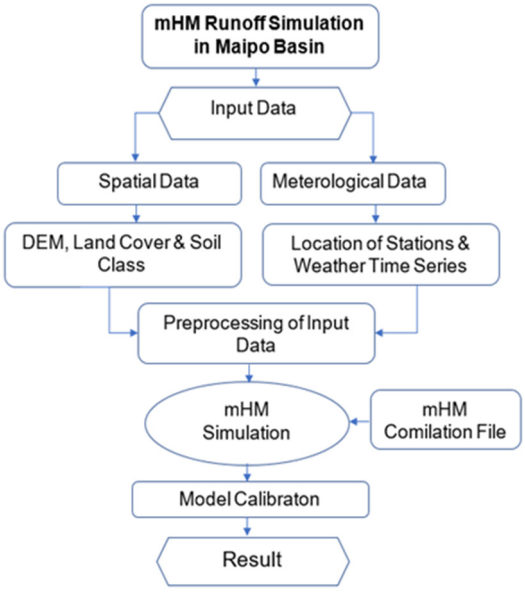

Figure 6. mHM Workflow.

2.4. MATILDA – (Modeling Water Resources in Glacierized Catchments) MATILDA - Modeling Water Resources in Glacierized Catchments (https://github.com/ cryocoolers/matilda) model aims to provide an open-source tool that allows users to assess the characteristics of small and medium-sized glacierized catchments, as well as estimate future water resources based on scenarios of climate change. To compute glacial melt, the MATILDA framework combines a simple positive degree-day routine (DDM) with the hydrological bucket model HBV [36].

Figure 7 illustrates the workflow of the MATILDA model, in the first part, input data is preprocessed to use in the pypdd tool model and HBV model. To calculate glacial melt using a positive degree-day method, MATILDA employs a modified version of the pypdd tool. It also modifies HBV from the Lumped Hydrological Models Playground (LHMP). The output includes numerous displays of the input and output data as well as the modeled time series for various water

Preprints (www.preprints.org) | NOT PEER-REVIEWED | Posted: 28 June 2023 doi:10.20944/preprints202306.1979.v1

balance components, basic statistics for these variables, and a choice of model efficiency coefficients (e.g., NSE, KGE

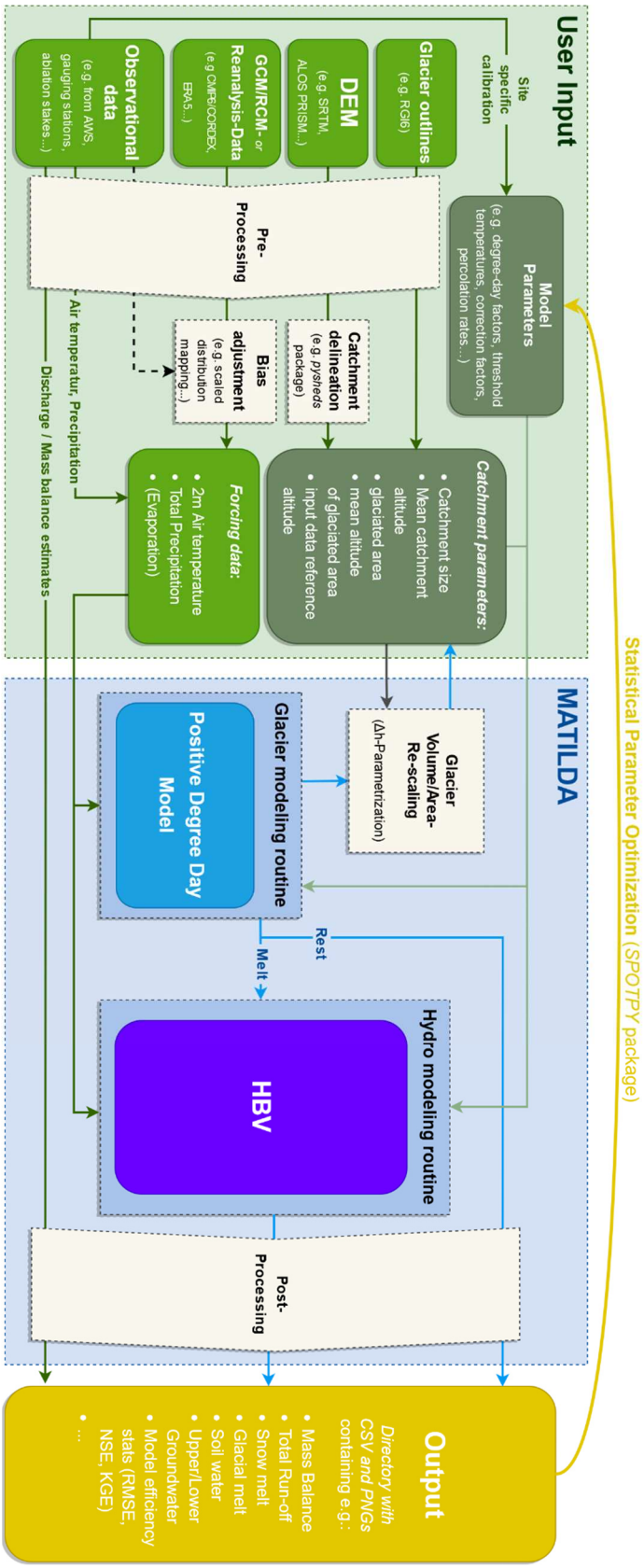

Figure 7. MATILDA Workflow (https://github.com/cryotools/matilda).

Preprints (www.preprints.org) | NOT PEER-REVIEWED | Posted: 28 June 2023 doi:10.20944/preprints202306.1979.v1

2.4.1. Pypdd

The Pypdd model [37] simulates glacier surface mass balance using a positive degree-day model in Python. A simple model is provided here that computes glacier accumulation and melt based on near-surface air temperatures and precipitation records. PDD is a method developed by Reeh [38] based on an empirical relationship between surface melt and temperature. During the model simulation, a normal distribution of temperature is assumed around the mean, as well as the possibility of melted snow and ice deposited on the surface of glaciers being re-frozen. Surface melt is commonly parameterized using the positive degree-day model for its simplicity [39]. A melting rate proportional to the number of positive degrees-days, which is equal to the integral of the temperature (T) over a time interval(A):

$$PDD = \int_0^A \max\left(T(t), 0\right) dt. \quad (8)$$

The difference between snowfall and rain is determined by a threshold temperature, the threshold temperature of rain is calculated as

$$T(rain) = T(snow) + T(diff) \quad (9)$$

Where T (snow) is the temperature below which all precipitation is solid and T (diff) is the difference between the T (snow) and temperature above which all precipitation is liquid. Between T (snow) and T (diff) fractions of liquid and solid precipitation change linearly (°C). The ice melt factor is calculated as

$$CFMAX(snow) = CFMAX(ice) + CFMAX(rel) \quad (10)$$

CFMAX (ice) is the ice melt rate (mm/day per K above freezing point) and CFMAX (rel) is the constant factor to calculate the snow melt rate from CFMAX(snow). Precipitation is separated into liquid and solid fractions based on linear transitions between threshold temperatures.

$$T_{reduce} = \frac{T(rain) - T2}{T(rain) - T(snow)} \quad (11)$$

Where T_reduce is calculated to use as a snow fraction by using threshold temperature and T (snow) and air temperature of the glacier (T2). Following that, snow melt is calculated by multiplying snow fraction by total precipitation (RRR). Rain results from the difference between precipitation and snow. Calculation of the melt rate is based on snow precipitation and positive degree day sums, and calculation of snowmelt is based on the number of positive degree days and attribute CFMAX (snow). If all the snow has melted and some energy remains (PDD), the ice melt is calculated using CFMAX (ice).

$$Pot(snow\_melt) = CFMAX(snow) * PDD \quad (12)$$

and, ice melt is proportional to excess snow melt.

$$Ice_{melt} = \frac{[Pot(snow\_melt) - Snow_{melt}] * CFMAX(ice)}{CFMAX(snow)} \quad (13)$$

Where Snow_melt is calculated by taking the minima of Snow and Pot (snow_melt). Accumulation, snow, ice melt, and runoff rate from the glaciers are calculated by using the Degree Day Model [37]. Total melt is calculated by adding snow melt and ice melt.

$$Total_{melt} = Snow_{melt} + Ice_{melt} \quad (14)$$

The total runoff rate is calculated as the difference between the total melt and fraction of meltwater that refreeze in the snowpack and the fraction of ice melt refreezing.

$$\text{Runoff}_{\text{rate}} = Total_{melt} - \text{refr}_{\text{snow}} - \text{refr}_{\text{ice}} \quad (15)$$

A list of parameters used as input in the MATILDA model is shown in Table 9. Depending on the catchment, the parameter ranges are further constrained based on available information. An evapotranspiration correction factor is set to be 0 as evapotranspiration data is available from the mHM results, if in case evapotranspiration data is not available Oudin formula calculates evapotranspiration values. In this analysis, linear lapse rates are used to scale the forcing data to the mean glacier elevation and the mean catchment elevation, respectively.

Preprints (www.preprints.org) | NOT PEER-REVIEWED | Posted: 28 June 2023 doi:10.20944/preprints202306.1979.v1

Para-meters	Description	Range	Unit
lr_temp	Lapse rate of air temperature	[-0.01, -0.003]	(K/m)
lr_prec	Lapse rate of precipitation	[0, 0.002]	(mm/m)
BETA	The parameter that determines the relative contribution to runoff from rain or snowmelt	[1, 6]	
CET	Evaporation correction factor	[0, 0.3]	
FC	Maximum soil moisture storage	[50, 500]	
K0	Recession coefficient for surface soil box (upper part of SUZ)	[0.01, 0.4]	
K1	Recession coefficient for upper groundwater box (the main part of SUZ)	[0.01, 0.4]	
K2	Recession coefficient for lower groundwater box (whole SLZ)	[0.001, 0.15]	
LP	The threshold for reduction of evaporation (SM/FC)	[0.3, 1]	
MAXBAS	Routing parameter, order of Butterworth filter	[2, 7]	
PERC	Percolation from soil to upper groundwater box	[0, 3]	
UZL	Threshold parameter for groundwater boxes runoff	[0, 500]	(mm)
PCORR	Precipitation (input sum) correction factor	[0.5, 2]	
TT_snow	Temperature below which all precipitation is solid. Between TT_snow and TT_rain fractions of liquid and solid precipitation change linearly	[-1.5, 2.5]	(°C).
TT_diff	Difference of TT_snow and temperature above which all precipitation is liquid (TT_rain).	[0.2, 4]	(°K)
CFMAX_ice	Ice melt rate (mm/day per K above freezing point).	[1.2, 12]	
CFMAX_rel	Factor to calculate snow melt rate from CFMAX_ice	[1.2, 2.5]	
SFCF	Snowfall Correction Factor	[0.4, 1]	
CWH	Fraction (portion) of meltwater and rainfall which retains in the snowpack (water holding capacity).	[0, 0.2]	
AG	Calibration parameter for glacier storage-release scheme. High values result in a small reservoir and instant release. Low values extend storage and delay release.	[0, 1]	
RFS	Fraction of meltwater that refreezes in the snowpack.	[0.05, 0.25]	
pfilter	Threshold above which precipitation values are elevation scaled using lr_prec. This addresses the common issue of reanalysis data to overestimate the frequency of low precipitation events. Handle with care! Should be fixed depending on the input data before parameter optimization.	[0, 0.5]	

2.4.2. Glacier retreat model

To calculate glacier area evolution in the study period, Huss and Hock 2015's [26] introduce Δh parameterization which is included in the degree-day routine (DDM) routine. As a data frame, the routine needs the initial glacier profile containing the spatial distribution of ice over elevation bands at the beginning of the study period. This Δh parametrization routine is based on the workflow outlined in Seibert et al. [40]. In response to a change in mass balance, Δh-parameterization describes the spatial distribution of glacier surface elevation variation. It is an empirical approximation method to characterize the glacier retreat at the scale of a particular glacier and is subject to uncertainty and several limitations. Huss et al. [41] originally developed this approach for periods dominated by

Preprints (www.preprints.org) | NOT PEER-REVIEWED | Posted: 28 June 2023 doi:10.20944/preprints202306.1979.v1

negative mass balances and glacier retreat. This is a more efficient state-of-the-art alternative to more complex glacier evolution models. For glacier mass changes to be translated into glacier area changes, a single-valued relationship needs to be established. In the model, this relationship is represented by a lookup table, which provides glacier areas for the different elevation zones based on a specific glacier mass value.

A glacier's volume can be calculated by integrating its initial glacier profile, which is a graphical representation of the area and thickness of a glacier (measured in mm water equivalent).

$$\mathrm{M} = \sum_{\mathrm{i}=1}^{\mathrm{N}} \mathrm{a_i}.\mathrm{h_i} \qquad (16)$$

Where, M is the total glacier mass in mm water equivalent relative to the entire catchment area, and for each elevation band i, a_i the area (expressed as a proportion of the catchment area) and water equivalent h_i in mm. The normalized elevation $E_{i,n}$ for each elevation band is derived from the absolute elevation of the corresponding elevation band i, as well as the maximum and minimum elevations of the glacier, E_{max} and E_{min}.

$$\mathrm{E_{i,n}} = \frac{\mathrm{E_{max}} - \mathrm{E_i}}{\mathrm{E_{max}} - \mathrm{E_{min}}} \qquad (17)$$

For each of the normalized elevations, the normalized water equivalent change is calculated using the following function (Huss et al., 2010).

$$\Delta \mathrm{h}_i = (E_{i,n} + a)^{\gamma} + b(E_{i,n} + a) + c, \qquad (18)$$

where $\Delta \mathrm{h}_i$ is the normalized (dimensionless) ice thickness change of elevation band i and a, b and c, and γ are empirical coefficients. These empirical coefficients are based on the glacier size class. If the glacier area is greater than 20 km^2 then a = -0.05, b = 0.19, c = 0.01, and y = 4 are chosen by Huss et al. [41]. Glacier volume balance change ΔM is computed by using a scaling factor f_s (mm) which scales the dimensionless Δh, and the glacier mass with normalized water equivalents change for each of the elevation bands.

$$\Delta M = f_s \cdot \sum_{i=1}^{N} a_i . \Delta h_i \qquad (19)$$

$$\boldsymbol{f_s = \frac{\Delta M}{\sum_{i=1}^{N} a_i . \Delta h_i}} \qquad (\mathbf{20})$$

For each elevation band, the new water equivalent $h_{i,t+1}$ is computed starting from the user-specified initial glacier thickness profile for t=0 as

$$\mathbf{h_{i,t+1} = h_{i,t} + f_s \Delta h_i} \qquad (\mathbf{21})$$

In this equation, $h_{i,t}$ represents the water equivalent of elevation band i after reducing the glacier mass t times by ΔM. After the new water equivalent values for each elevation zone have been computed, the glacier area is updated accordingly. It is common for glaciers at elevations to have uneven distributions of ice, with thinner ice layers along their edges. This uneven distribution results in a reduction in area, so a simplified representation of glacier geometry is used to scale the area within certain elevation bands (Eq. 7) based on Bahr et al. [42] and Huss and Hock [26], which also applies relationship between glacier width and glacier thickness:

$$\mathbf{a_{i,scaled} = a_i \left(\frac{h_i}{h_{i,initial}} \right)^{0.5}} \qquad (\mathbf{22})$$

A reduction in glacier area over elevation was observed because of the combination of Δh parameterization (Eqs (16) through (21)) with glacier width scaling (Eq. 22). As a result of this, the glacier area and glacier mass relationship is stored in a lookup table in steps of 1 percent of the initial glacier mass.

 doi:10.20944/preprints202306.1979.v1

2.4.3. Matilda Data Preparation and Initializations

ArcGIS tool is used to extract spatial information from the Maipo catchment and glaciers by using geo-processing tools for analyzing, editing, and converting data. For creating a Glacier profile of a glacier, area, and water equivalent per elevation band are required. The following steps are followed to create the input file for the MATILDA model.

Firstly, several glaciers are selected for individual basins which are available as ice thickness raster data, and then all non-available number (NAN) of rater data is removed and merged into one raster file. Each basin raster is extracted individually and merged into one by using SRTM raster data and vectorized polygon. Contour is created by using merged glacier raster data with 10m of elevation band and then zonal statistics as the table is created by using a contour vectorized polygon of the glacier and ice thickness data.

To run a Matilda model, several required input variables are prepared by using CAMEL-CL data sources. Input variables such as air temperature (°C), total precipitation (mm), and (if available) evapotranspiration data (mm). To calibrate the model, runoff observations are used, units of runoff change from $m^3\ s^{-1}$ to mm/day, and all data sets are prepared as daily resolutions. Matilda offers glacier modeling as an optional option to include the Δh parameterization from Huss and Hock [26] within the DDM routine and to calculate glacier area evolution during the study period. To conduct the routine, an initial glacier profile is created, which contains the spatial distribution of ice over elevation bands at the beginning of the study period.

- Elevation - elevation of each band with a resolution of 10 m.
- Area - an area of each band as a fraction of the total glacier area
- WE - ice thickness in mm w.e.
- EleZone - combined bands over 100-200 m.

A base contour is used with a 10m resolution starting with the lowest elevation of the glacier. The glacier ice thickness raster file is used to create the zonal statistics for all the bands available for the glaciers. The area is extracted from the zonal statistics table for each elevation band and the unit is changed from m^2 to km^2. The thickness of a glacier is converted to grams of water equivalents (mm) by applying an ice density of 906 kilograms. A mass balance term is expressed as water equivalents (w.e.) to allow comparisons to be made between different glaciers. In a snow or ice melting scenario, the water equivalent represents the volume of water that is produced by the glacier.

The MATILDA package comprises four different modules such as parameter setup, data preprocessing, simulation core, and post-processing. A complete workflow can be used via the MATILDA_simulation function or through the individual modules as well. To use the MATILDA_simulation function, the following steps are followed to accomplish the run.

After downloading and installing all the dependencies of MATILDA, spin-up and simulation periods are defined with one year of spin-up. Catchment properties such as catchment area, glacierized area, average elevation, and average glacier elevation are specified. The output frequency is defined as daily. (Option: daily, weekly, monthly, or yearly). Using the MATILDA_parameter function parameters are specified and if no parameters are specified, default values are applied. MATILDA_preproc function is run to use the data preprocessing. MATILDA_submodules function is used to run the actual simulation. MATILDA_plots function is used to plot the runoff, meteorological parameters, and HBV output variables using.

For running the MATILDA model, the MATILDA package, dependencies and other following python library is installed (Xarray, numpy, pandas, matplotlib, scipy, datetime, hydroeval, HydroErr, and Plotly). Figure 8 shows the workflow of the mHM and MATILDA melt model. For preparing the MATILDA melt file, a text file is prepared from the output result of the MATILDA on hourly bases to run into the mHM model. All the model files including input and output results available as shown in Table 21 Digital Appendix.

Preprints (www.preprints.org) | NOT PEER-REVIEWED | Posted: 28 June 2023 doi:10.20944/preprints202306.1979.v1

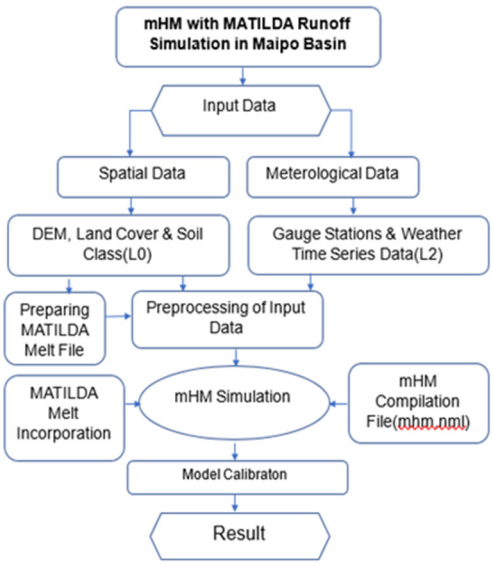

Figure 8. MATILDA Workflow (https://github.com/cryotools/matilda).

2.4.4. Calibration and Criteria

To evaluate the calibration parameters and to analyze results in the following chapters, a variety of statistical measures is employed. A summary of the measures used in this thesis can be found here, whereas Krause et al. [43] provide a more comprehensive discussion of each measure and alternative measures. The parameters of runoff models are traditionally calculated by calibrating against observed runoff and not by verifying internal model variables. Because of this, there may be a chance of compensating for errors [44], and it may well be the case that the model performs well concerning runoff, even with an incorrect snow or ice distribution.

Many studies use the coefficient of determination for multivariate scenarios, or r^2 and it provides a dimensionless value between 0 and 1, where 1 represents the optimum performance of the model. And can be calculated as

$$r^2 = \left(\frac{\sum_{t=1}^{T} (Q_o^t - \overline{Q_o})(Q_m^t - \overline{Q_m})}{\sqrt{\sum_{i=1}^{n} (Q_o^t - \overline{Q_o})^2} \sqrt{\sum_{i=1}^{n} (Q_m^t - \overline{Q_m})^2}} \right)^2 \qquad (23)$$

where:

$\boldsymbol{Q_m^t}$ = model discharge at time t

$\boldsymbol{Q_o^t}$ = is the observed discharge at time t$\boldsymbol{\overline{Q_o}}$= average runoff during the calculation period

n = number of days in the calculation period

A widely used specification for the NSE criterion of runoff developed by Nash and Sutcliffe [45] is widely used in the calibration and evaluation of rainfall-runoff models. Its value ranges from -∞ to 1, if the simulated runoff value is greater than zero, the simulated runoff represents a good observable representation of actual runoff variations better than the observed long-term average.

$$\mathbf{NSE = 1 - \frac{\sum_{i=1}^{n} (Q_0^t - Q_m^t)^2}{\sum_{i=1}^{n} (Q_o^t - Avg(Q_o))^2}} \qquad (\mathbf{24})$$

The Root Mean Square Error (RMSE) reveals the mean difference between modeled Q_m^t and observed Q_o^t discharge:

$$\mathbf{RMSE = \sqrt{\frac{\sum_{i=1}^{n} (Q_m^t - Q_o^t)^2}{n}}} \qquad (\mathbf{25})$$

The advantage of using this method is that it preserves the units of the original data, so measurements can be compared to see the magnitude of errors, not just the model's performance.

Preprints (www.preprints.org) | NOT PEER-REVIEWED | Posted: 28 June 2023 doi:10.20944/preprints202306.1979.v1

RMSE values approaching zero represent a better agreement between observations and predictions, but, likewise r^2, it has a limitation due to its large bias toward outliers.

The model execution of the Matilda applications is here evaluated with the modified Kling-Gupta Efficiency (KGE) [46]:

$$\mathbf{KGE} = \mathbf{1} - \sqrt{(\mathbf{r}-\mathbf{1})^2 + (\boldsymbol{\beta}-\mathbf{1})^2 + (\boldsymbol{\gamma}-\mathbf{1})^2} \qquad (\mathbf{26})$$

where,

r = Pearson Correlation Coefficient

$$\boldsymbol{\beta} = \left(\frac{\boldsymbol{\mu_{sim}}}{\boldsymbol{\mu_{obs}}}\right)^2$$

$$\boldsymbol{\gamma} = \left(\frac{\boldsymbol{\sigma_{sim}/\mu_{sim}}}{\boldsymbol{\sigma_{obs}/\mu_{obs}}}\right)^2$$

Where μ_{obs} is the mean of observed values, μ_{sim} is the mean of simulated values, σ_{sim} is the standard deviation of simulated values and σ_{obs} is the standard deviation of observed values. KGE = 1 means an ideal match between simulated and observed values, and KGE ≈ -0.41 indicates the model simulation is as accurate as the observed mean (Knoben et al., 2019. For analysis mHM and Matilda model KGE, NSE, and RMSE model efficiency coefficients are employed by using the "HydroErr" library [47].

3. Results

3.1. mHM Results

At first, mHM (mesoscale hydrological model) is executed for the Maipo basin by using prepared forcing data such as mean temperature, precipitation, and evapotranspiration also with morphological data for spatial discretization with a hydrological resolution of 0.0625-degree decimal. The model is run daily from 1950 to 2020 and calibrated with observed discharge data. Model mHM results from 1950-2020 showed that the approach was viable, as illustrated by Kling-Gupta's Efficiency of 0.80 and Nash-Sutcliffe Efficiency of 0.70. However, the model performed well even though some missing values were present in the observed data, mHM model overestimation occurs especially during the late summer season when temperature decreases, and some missing values are present in the observed data. mHM, the model is also run monthly to compare with the daily data. Calibration with NSE and KGE daily temporal shows better results as compared to the monthly output result from the mHM model according to Table 10.

Table 10. Observed and mHM simulation Stream flow calibration results on a daily and the monthly basis from 1950 to 2020.

Calibration parameters	Daily	Monthly
	Qobs/Qsim	Qobs/Qsim
$\mathbf{r^2}$	0.26	0.30
NSE	0.70	-0.24
KGE	0.80	0.65

During the 1950 to 2020 period, the mean daily observed discharge was 112.22 m^3s^{-1}, and mHM was calculated at 95.06 m^3s^{-1}. The minimum observed discharge was recorded in July 2019 and the maximum was in May 1991, while mHM calculated the minimum in August 1950 and maximum in January 1998 as 4.98 and 530.35 m^3s^{-1} respectively.

For further analysis and comparison of the simulated flow processes to the observed ones, two periods of time are selected 2011-2014 and 2015 to 2018 performed individually with one year of the warm-up period. Model calibration was pursued by optimization of three goodness of fit measures, namely r^2 (Coefficient of Determination), NSE (Nash-Sutcliffe Efficiency), and KGE (Kling-Gupta Efficiency), these statistical indices values were used to compare the simulated and observed daily runoff values. The stream flow calibration results are given in Table 11 from 2012-2014 and 2016-2018, and warm-up periods were excluded from statistical analysis.

Preprints (www.preprints.org) | NOT PEER-REVIEWED | Posted: 28 June 2023 doi:10.20944/preprints202306.1979.v1

Table 11. Observed and mHM simulation Stream flow calibration results daily from 2011-2014 and 2015-2018.

Calibration parameters	2011-2014	2015-2018
	Qobs	Qsim
r^2	0.007	-0.21
NSE	0.40	0.15
KGE	0.70	0.53

KGE values for 2011-2014 are 0.70 and for 2015-2018 0.53, 2011-2014 showed a good result as compared to 2015-2018, also NSE and manually calculated Coefficient of determination values are 0.40 and 0.007 respectively according to Table 11, indicating a good agreement between simulated and observed runoff for 2011-2014. Daily calibration of mHM runoff results for 2015-2018 is showing poorly because they have a high peak during the 2016 autumn season as shown in Figure 10.

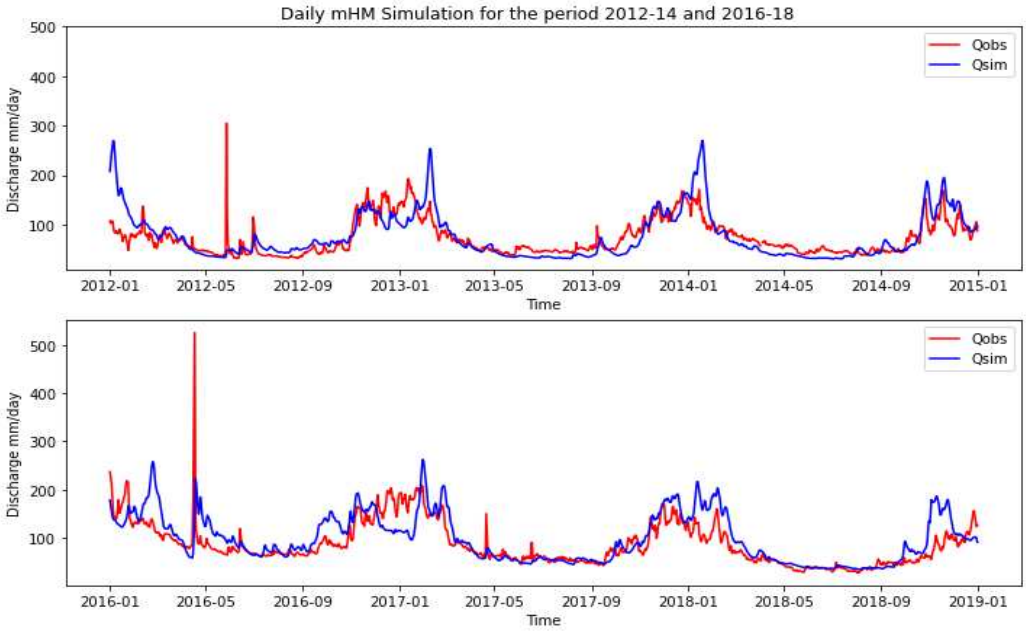

Figure 10. mHM simulation (Qsim, blue) and observed stream flow (Qobs red).

Figure 10 represents daily mHM simulation for the period of 2012-2014 and 2016-2018. mHM in blue color are underestimated during the 2012-2014 period and in 2016-18 both almost followed the same path except during seasonal transition. A closer investigation of the daily runoff dynamics for the Maipo basin shows that large early summer peaks are underestimated in the simulation results except in 2018, while other peaks are slightly overestimated. In autumn 2012 and 2016 there was an extreme flood of observed runoff, which was underestimated by mHM in 2012, and shows a small peak in 2016.

The general overview of the observed and simulated stream flow data is given in Table 12. For both observed and simulation mean, minimum, maximum, and standard deviation were calculated. According to Table 12, the observed stream flow is higher than the mHM simulated stream flow although in 2016-2018 the daily mean discharge is very small as compared to the period 2016-2018. The discharge rate is lower in 2014-2016 but the maximum discharge attained in a day is higher than in 2016-2018. The maximum peak of stream flow is not able to be attained by the mHM model in both time durations.

Table 12. mHM Descriptive statistics for Daily streamflow (m^3s^{-1}).

	2012-2014		2016-2018	
Mean	70.61	62.53	88.69	87.16

Preprints (www.preprints.org) | NOT PEER-REVIEWED | Posted: 28 June 2023 doi:10.20944/preprints202306.1979.v1

Min	28.1	14.03	26.3	15.63
Max	305	265.91	526	258.11
Std	33.51	46.42	46.19	50.97

There are four seasons in Chile, summer runs from December to February (DJF), autumn from March to May (MAM), winter from June to August (JJA), and spring from September to November (SON).

A comparison of observational and simulation statistics is also presented in Table 13; these statistics demonstrate how the flow differs throughout the season. There is a higher average runoff both in the observed and simulated summer seasons, while the lowest mean runoff is found in the autumn season. A minimum runoff was also found in the Autumn season both in recorded and simulated data. Model mHM shows a huge gap between the minimum runoff in the summer season, also same with maximum observed discharge recorded an unanticipated maximum runoff in winter as 526 m^3s^{-1}, while mHM simulated only a maximum of 214.90 m^3s^{-1}. Seasons with high runoff, such as summer and Spring, show high standard deviations and among all of them spring mHM simulation has the highest standard deviations.

Table 13. Descriptive statistics for Seasonal runoff (m^3s^{-1}) from 2012-2018.

	Summer		**Autumn**		**Winter**		**Spring**	
	Qobs	**Qsim**	**Qobs**	**Qsim**	**Qobs**	**Qsim**	**Qobs**	**Qsim**
Mean	125.88	130.95	49.61	42.62	65.87	57.52	81.73	89.76
Min	48.6	37.30	26.3	26.44	28.1	20.64	40.5	31.97
Max	237	265.91	119	96.51	526	214.90	175	191.85
Std	35.98	46.38	13.24	14.56	31.73	34.35	32.85	44.14

A spatially distributed mHM output file is transformed into a one-dimensional mean for both periods of data for plotting and visualization. Model mHM calculated temporal variability of actual evapotranspiration, soil moisture, depth of snowpack, snow melt, and unsaturated storage represented in Figures 11 and 12 from 2012 to 2018. As the graph shows, actual evapotranspiration and snowpack exhibit seasonality, and a phase shift occurs between actual evapotranspiration and snowpack when snowpack reaches its peak after winter and actual evapotranspiration during summer. Additionally, there is a phase shift between snowmelt and snowpack, with the fastest snowpack decrease occurring when snowmelt is at its peak.

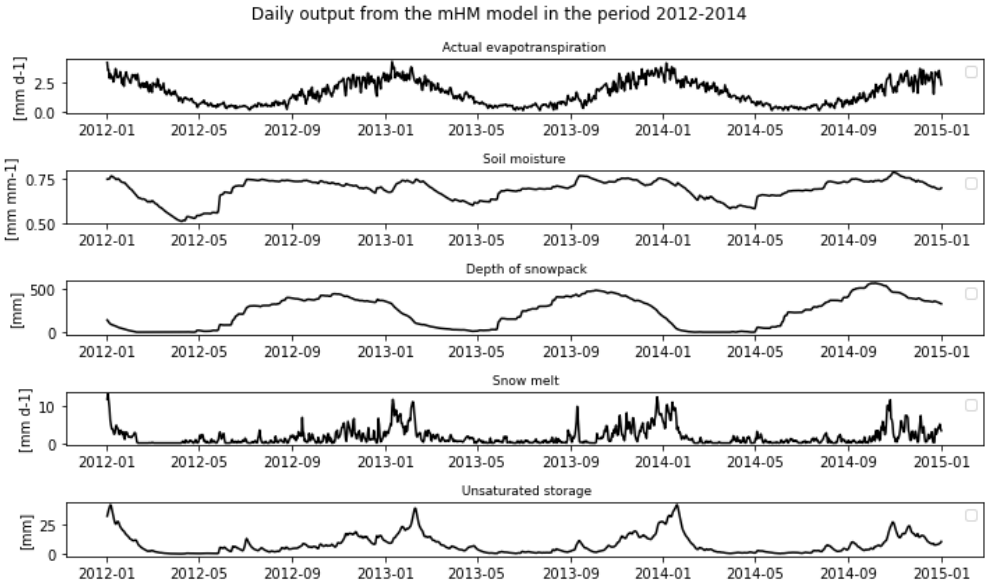

Figure 11. mHM Model Output (Actual evapotranspiration, Soil moisture, Depth of snowpack, Snowmelt, and Unsaturated storage) for 2012-2014.

Preprints (www.preprints.org) | NOT PEER-REVIEWED | Posted: 28 June 2023 doi:10.20944/preprints202306.1979.v1

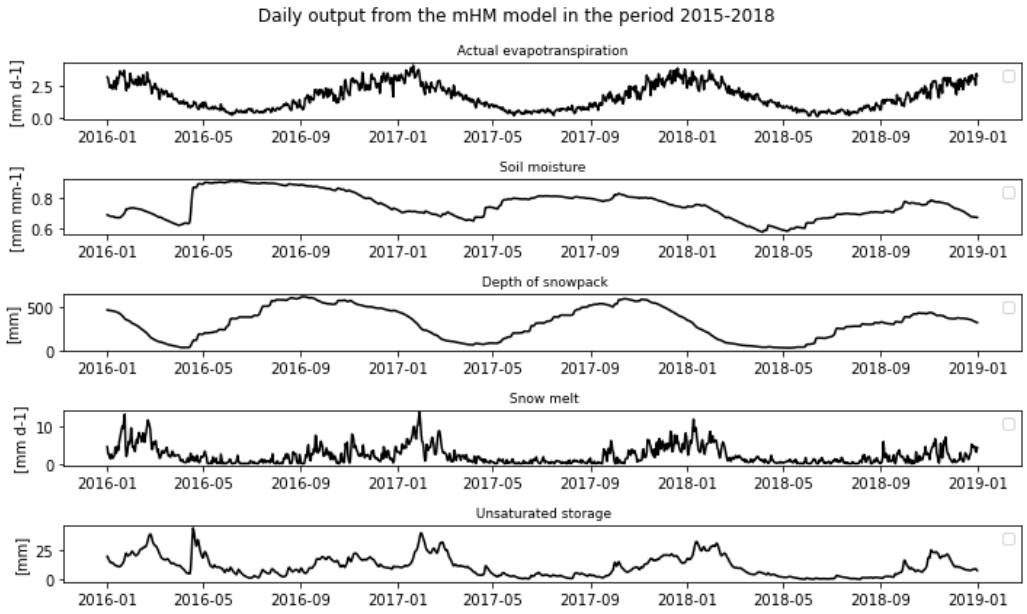

Figure 12. mHM Model Output (Actual evapotranspiration, Soil moisture, Depth of snowpack, Snowmelt, and Unsaturated storage) for 2016-2018.

Descriptive statistics of mHM model output are determined by combining both periods. The mean of actual evapotranspiration and snow melt is 1.59 mm/day and 1.91 mm/day respectively. In terms of snowpack and unsaturated storage, the average depths are 261.43 mm and 9.15 mm, respectively. The meaning of actual evapotranspiration and snow melt is 1.59 mm/day and 1.91 mm/day respectively. In terms of snowpack and unsaturated storage, the average depths are 261.43 mm and 9.15 mm, respectively. The maximum and minimum of actual evapotranspiration is 4.19 mm/day and 0.003 mm/day, while snowmelt has 13.63 mm/day and 0. Moisture levels in the Maipo basin generally range from 0.51 to 0.91 mm/mm, with a mean of 0.70 mm/mm according to Table 14.

Table 14. Descriptive statistics of mHM Model Output (Actual evapotranspiration, Soil moisture, Depth of snowpack, Snowmelt, and Unsaturated storage).

	Actual Evapotrans. (mm/day)	Soil moisture (mm/mm)	Depth of snowpack (mm)	Snow melt (mm/day)	Unsaturated storage (mm)
Mean	1.59	0.70	261.43	1.91	9.15
Min	0.003	0.51	0	0	0.037
Max	4.19	0.91	679.42	13.63	43.88
Std	1.0	0.08	194.37	2.37	8.53

4.2. MATILDA Models' Performance

4.2.1. Matilda runoff for Maipo basin

To run a MATILDA model, a forcing file is prepared from the daily meteorological input parameters, and runoff data from CAMELS-CL is used to calibrate the model. Glacier profile data such as area per elevation band and water equivalent is prepared from the ice thickness raster file and converted into the required units. Every glacier in the basin individually preprocesses and small glaciers having less than 5 km^2 of areas were neglected in the study. After setting up all the parameters and catchments properties, the MATILDA model is performed from 2011-2014 and 2015-18, with one year of data set for the warm-up period. In the MATILDA model, the simulated and observed daily runoff values were compared using three goodness of fit measures: Nash-Sutcliffe efficiency (NSE) and Kling-Gupta efficiency (KGE). Table 15 shows daily runoff calibration results

Preprints (www.preprints.org) | NOT PEER-REVIEWED | Posted: 28 June 2023 doi:10.20944/preprints202306.1979.v1

from 2012-2014 and 2016-2018, excluding warm-up periods. Models from 2016-18 perform better with 0.44 KGE values versus models from 2012-14 with 0.41 KGE values. In contrast, results for 2012-2014 show better calibration by NSE. The monthly calibration of MATILDA runoff is showing better results than daily runoff values, as given in Table 15. In 2016-2018 it improved more as compared to the 2012-14 and overall MATILDA model performance is on average.

Table 15. Observed and MATILDA model daily and monthly runoff calibration from 2012-2014 and 2016-2018.

	Daily				Monthly			
Calibration	**2012-2014**		**2016-2018**		**2012-2014**		**2016-2018**	
parameters	**Qobs**	**Qsim**	**Qobs**	**Qsim**	**Qobs**	**Qsim**	**Qobs**	**Qsim**
NSE	0.25		0.20		0.38		0.42	
KGE	0.41		0.44		0.56		0.62	

Figure 13, reports the flow contribution (mm/day) as catchment runoff in blue, glacier runoff in magenta color, and the top of that total runoff in black line, indicating the flow generation mechanism from 2012-14 and 2016-18 and, observed runoff from CAMELS CL is used shown in red line for calibrating the runoff. From 2012 to 2018, MATILDA reproduced reasonably well during the summer season with huge melts from glaciers except early in 2012 with high runoff during the Chilean summer. MATILDA simulations have a sudden large fall all of the year, especially after the late Spring season. Mostly glacier melt produces water that contributes to flow during summer and autumn and precipitation peaks toward the middle of the year.

The average of 3 years as a mean annual data is also shown in figure 13 in the small square, which is illustrated from 2012-14 and 2016-18 with a monthly x-axis, most of the glacier melt happens at the beginning and at the end of the year, catchment runoff is higher in the mid of the year. A substantial amount of melt was produced by the glacier in April and May of 2018, which was not evident in the observed data, however suddenly, MATILDA stopped melting at the end of June, and thus glacier runoff dropped immediately due to the phase change.

According to Tables 16 and 17, the yearly average runoff during 2012–2014 & 2016-2018 from MATILDA is 1.331 mm/day and 1.56 mm/day. In 2012-2014 glacier melts contributed more than twice to the catchment runoff without having glaciers. In 2012-14 total mean runoff is less than the observed runoff because the basin-wide annual mean runoff contribution decreased by 31% from 2012 to 2014 in the MATILDA simulation. According to the mean annual temperature forcing data, there is 0.61 C° of loss from 2012 to 2014. The mean snow melt was 0.35 mm/day and 0.57 mm/day during 2012-2014 and 2016-2018, with the maximum being 18.688 mm/day in September 2016 for the whole period. Compared to 2012-2014, glacier runoff and without glacier runoff are higher in 2016-2018.

Preprints (www.preprints.org) | NOT PEER-REVIEWED | Posted: 28 June 2023 doi:10.20944/preprints202306.1979.v1

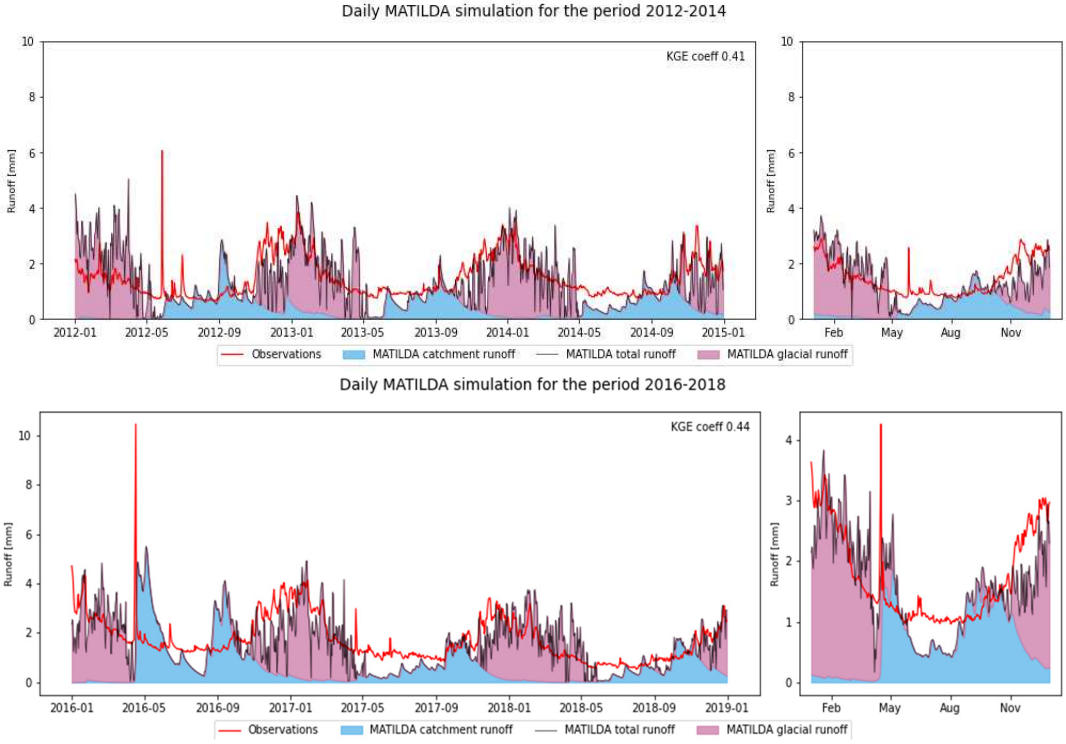

Figure 13. MATILDA Runoff Simulation with observation from 2012-14 and 2016-18.

Table 16. Descriptive statistics for Runoff(mm/day) from 2012-2014.

	Snow Melt (mm/day)	Runoff Catchment (mm/day)	Runoff Glaciers (mm/day)	Total Runoff (mm/day	Observed Runoff (mm/day)
Mean	0.35	0.435	0.896	1.331	1.466
Min	0	0	0	0.023	0.644
Max	14.76	2.857	5.033	5.047	6.059
Std	1.45	0.428	1.117	0.981	0.7

Table 17. Descriptive statistics for Runoff(mm/day) from 2016-18.

	Snow Melt (mm/day)	Runoff Catchment (mm/day)	Runoff Glaciers (mm/day)	Total Runoff (mm/day	Observed Runoff (mm/day)
Mean	0.57	0.646	0.917	1.563	1.734
Min	0	0	0	0.013	0.522
Max	18.688	5.399	4.824	5.497	10.45
Std	2.06	0.877	1.158	1.132	0.898

From 2012-14, MATILDA glacier runoff produced 67% of the total runoff and 58% by 2016 to 2018 time periods. Overall, in 2016-2018 the mean snowmelt and runoff is higher as compared to 2012-2014.

Significant glacier area reduction was found by Δh parameterization approach during the simulation period of 2012-14 and 2016-2018, glacier area is reduced by 22-23 % in both periods 2016-18. Despite more glaciers melting in 2016-18 than in 2012-14, the glacier area reduction percentage is not much different, because the model assumes the initial glacier profiles are equal, which is not the case. Besides local climate, glacier area decline is influenced by local topographic factors and glacier spatial distribution.

Preprints (www.preprints.org) | NOT PEER-REVIEWED | Posted: 28 June 2023 doi:10.20944/preprints202306.1979.v1

Table 18: Glacier Area and Elevation changes, 2012-14 (Δh parameterization).

2012-2014			2016-2018		
Time	**Glacier area (km^2)**	**Glacier Elevation(m)**	**Time**	**Glacier area(km^2)**	**Glacier Elevation(m)**
Initial	343.95	4351	**Initial**	343.95	4351
2012	288.96	4374	**2016**	295.27	4365
2013	279.06	4389	**2017**	282.43	4384
2014	266.30	4413	**2018**	268.24	4409

A seasonal comparison of observational and simulation statistics is also presented in Table 19. These statistics demonstrate how flows vary from season to season. Observed and simulated summer seasons experience higher mean runoff, while winter seasons experience the lowest mean runoff. A minimum runoff was also found in the Autumn season, by MATILDA simulated as 0.004 mm/day and after that autumn season as 0.007 mm/day. Model mHM shows a huge gap between the mean runoff in the winter season, as compared to the other season. Seasons with high runoff, such as Summer and Autumn, show high standard deviations and among all of them spring mHM simulation has the highest standard deviations.

Table 19. MATILDA Descriptive statistics observed and simulation Seasonal runoff(mm/day) from 2011-2018.

Unit	**Summer**		**Autumn**		**Winter**		**Spring**	
(mm/day)	**Qobs**	**Qsim**	**Qobs**	**Qsim**	**Qobs**	**Qsim**	**Qobs**	**Qsim**
Mean	2.33	2.158	1.23	1.191	0.944	0.543	1.543	1.294
Min	0.966	0.023	0.558	0.007	0.522	0.004	0.64	0.034
Max	5.523	4.506	10.45	5.047	2.364	3.164	3.47	5.372
Std	0.73	0.843	0.520	1.070	0.239	0.415	0.632	0.797

For the period 2012-2018, MATILDA calculated the temporal dynamics of actual evapotranspiration, soil moisture, water in the snowpack (without glaciers), and upper and lower groundwater boxes, as shown in Figures 14 and 15. According to the above graph, actual evapotranspiration has similar seasonal patterns, peaking during the summer and declining during the winter most of the time. The mean of actual evapotranspiration, soil moisture, and water in the snowpack is 0.777 mm/day, 72.39 mm and 23.6 mm respectively calculated from 2012 to 2018. Based on the initial soil conditions in the upper and lower groundwater zones, mean values for the upper and lower groundwater boxes were 2.377 mm and 8.69 mm respectively.

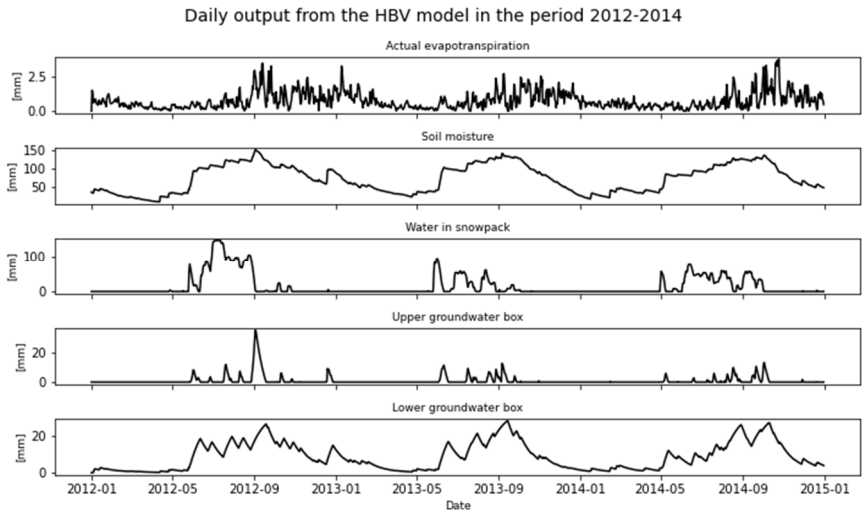

Figure 14. HBV Model Output (Actual evapotranspiration, Soil moisture, Water in the snowpack, Upper and Lower groundwater box) for 2012-2014

Preprints (www.preprints.org) | NOT PEER-REVIEWED | Posted: 28 June 2023 doi:10.20944/preprints202306.1979.v1

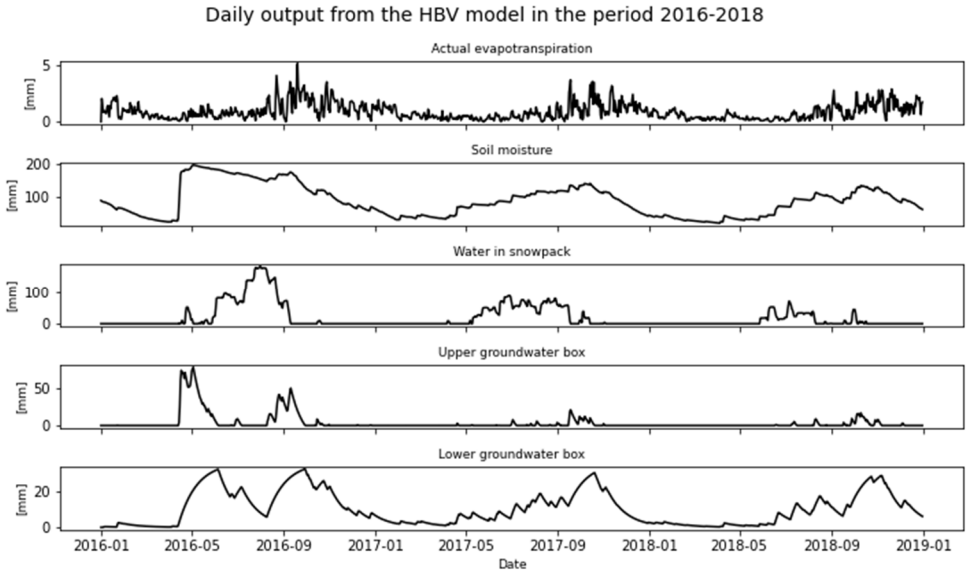

Figure 15. HBV Model Output (Actual evapotranspiration, Soil moisture, Water in snowpack, Upper and Lower groundwater box) for 2016-2018.

4.3. mHM with MATILDA Glacier Melt

To do further analysis to achieve the initial thesis goal, the MATILDA glacier melt is coupled with the mHM (mesoscale Hydrologic Model) to investigate whether this coupling can help better represent glaciers in glacierized basins and predict river discharge. The coupling was performed by adding the hourly resampled MATILDA glacier melt time series data to replace the snowmelt of the mHM grid cell. The melting of the Olivares sub-basin glacier for the period 2011-2018 is considered for testing purposes.

Figure 17 shows the runoff from 2011-18 of observed mHM and mHM_MAT melt. In 2011- 2015 there is a strong underestimation by the mHM_mat model, melting around 2012, both observation and mHM are out the same way, but the mHM_MAT at is decreasing much faster. During Summer time (December to February) mHM and mHM_MAT follow the same path, however, the mHM_MAT model underestimates mostly during the transition of the season. A similar, but not significantly larger, underestimate was made by the mHM_MAT model in 2014

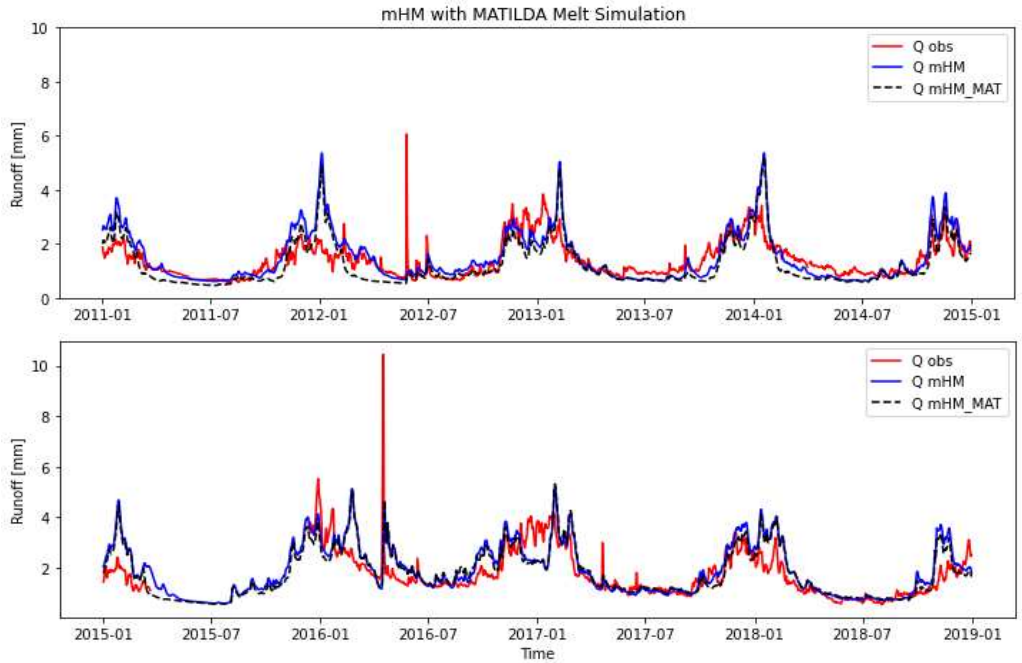

Preprints (www.preprints.org) | NOT PEER-REVIEWED | Posted: 28 June 2023 doi:10.20944/preprints202306.1979.v1

Figure 17. mHM, MATILDA, and mHM with MATILDA_Melt Observed Vs Simulation runoff.

In the following year, this difference will be almost nonexistent, and by 2016, they are almost equal in terms of growth. A visualization of the glacier melt of the sub-basin is shown in Figure 18 to examine the details of the new couple model. According to MATILDA's estimates from 2011-15 and 2015-18, the average total melt in the Olivares basin was 0.92 mm/day and 1.24 mm/day.

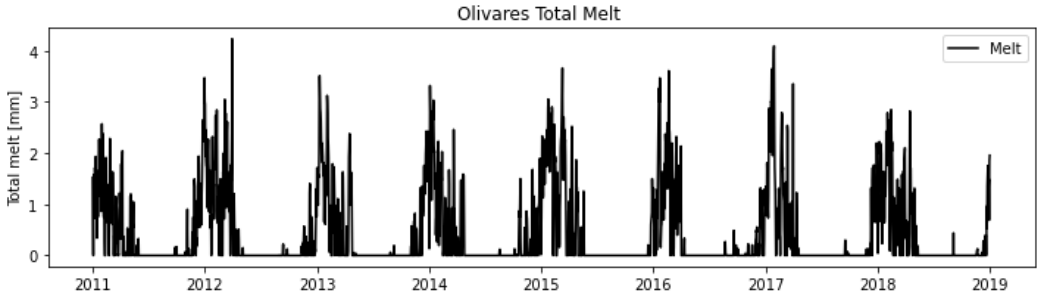

Figure 18. MATILDA Total melt of Olivares sub-basin.

The difference between the accumulation rate and the runoff rate, the average surface mass balance is higher in the 2011-15 period as compared to 2015-16. The glacier reservoir had a mean melt of 0.40 mm in 2011-15 and 0.42 in 2015-18. In the case of Matilda parametrization, the initial storage condition, actual glacier area, and elevation distribution is possibly underestimated, which leads to a significant part of the ablation period being missed. Model calibration is performed to analyze the model credibility by using three optimizations, the stream flow calibration results are given in Table 20 from 2012-2014 and 2016-2018, and warm-up periods were excluded from statistical analysis. In 2011-2015 NSE of the mHM model performing better as mHM_MAT have initial parameters underestimation. In the 2015-18 model, mHM_MAT is performing well by all optimization as observed data have some missing values. Olivares basin has only 20% of the total glacier, and the glacier has high altitudes and low temperatures because of that melt is very low and the model performs slightly differently overall.

Table 20. Daily streamflow calibration results.

Calibration para-meters	2011-2015		2011-2015		2015-2018		2015-2018	
	Qobs	QmHM	Qobs	QmHM_MAT	Qobs	QmHM	Qobs	QmHM_MAT
r^2	0.19		0.21		0.25		0.37	
NSE	0.57		0.49		0.14		0.19	
KGE	0.63		0.64		0.60		0.62	

4. Discussion

For the periods 2012-2014 and 2016-2018, the calibration of the mHM model for NSE is 0.40 and 0.15, whereas for MATILDA have 0.25 and 0.20. mHM is showing a good result for the first period and MATILDA has good results with NSE values. For KGE, observed and mHM simulation of stream flow is 0.70 and 0.53 for the period 2011-2014 and 2015-2018. Since the KGE values for the MATILDA model are 0.41 and 0.44 for the period 2011-2014, KGE values for mHM represent better results than those of MATILDA.

The daily mean streamflow (m^3 s^(-1)) calculated by mHM is less than the mean observed streamflow in both periods 2012-2014 and 2016-2018. In the MATILDA model mean runoff(mm/day) calculated is less than the observed mean flow, so both models have not reached the observed mean values (tables 10 and 13). mHM and MATILDA both models couldn't reach the maximum of the observed streamflow on any day of the simulation periods. In the summer and winter seasons mHM produces more average discharge than the observed average discharge. In the MATILDA model, in every season observed mean runoff is more than the simulated runoff. MATILDA produced well

during the summer season, except early in 2012 with high runoff due to Chilean summer. However, after late spring, there was a sudden decrease in simulation.

For the entire Maipo basin, the Matilda model is giving an average result. Mostly, in winter when there is no glacier runoff the model is poorly performed, seen in Figure 11. The catchment runoff contribution without glaciers varied by 31% during 2012-2014, but the contribution with glaciers was more than twice as large as without glaciers. The glacier melt is more in 2016-18 as compared to 2012-14 but the glacier area reduction percentage is not much different because it is assumed in the model that the initial glacier profile for both periods is the same, which is not in the real scenario. Individual sub-basin analysis was also performed with the mHM model and among all the basins, the Colorado and Yeso sub-basins have the highest and same KGE value of 0.36 (table 18) and, whereas Olivares and Upper Maipo basins have the lowest. The calibration result of mHM shows that the model is working very well even without having a glacier module, on the other hand, MATILDA is showing average results. Overall mHM model perform well especially in 2015-18 even though there are some missing values in observed data.

4.1. Limitations and Outlooks

This research study was carried out by using two datasets ERA5 and CAMELS-CL for mHM and MATILDA models. The mHM model uses grid-based datasets which are not available in the CAMELS dataset, whereas the MATILDA model can run with the ERA5 dataset by aggregating. The MATILDA model is subject to some uncertainty largely because of input parameterizations and is not suitable for a big catchment. Matilda's main drawback is that it uses HBV, which always requires parameter calibration, whereas mHM can always be applied. Some parameters are difficult to calibrate since they affect the calibration objectives indirectly, and can be readily compensated for by other more dominant parameters [48]. In the Maipo catchment, there are permafrost and rock glaciers which have not been modeled in the present study due to a lack of knowledge in the study case area. Because of the significantly smaller catchment area and the high data quality of the nearby glacier station, the results can be rated as satisfactory and generally better.

For further research, it is more appropriate to use the ERA5 dataset for both models so that better comparisons can be made. Model mHM and MATILDA both need 3 forcing data such as precipitation, temperature, and evapotranspiration and perform well with a degree day approach at the cost of limited data requirement, although they are not reliable in some cases when the radiation is too high at the top and a large portion of the melt will evaporate. The glacier can also melt at low temperatures because of the sunlight. Moreover, the algorithm used for glacier mass balance and retreat can be further improved by including solar radiation and topographic factors in the degree-day factors. In addition, glacier mass balance components can be modeled with an energy balance approach. Although, it is more accurate to use physically-based glacier models to estimate future glacier dynamics and the redistribution of glaciers and snow if the climatic and hydrological systems are not stable [6] (Hock, 2005). MATILDA as a lumped model did not work well during the phase transition from Autumn to Winter season, in this case, a fully distributed model (mHM) can improve the streamflow by adding glacier melt distribution over the glacier elevation bands including evident slope and elevation zone according to the aspect classes. Once enough input and validation data are available, the physical models can be developed and used in glacier modeling.

5. Conclusions

Generally, mHM mimics acceptably seasonal flow dynamics as compared to MATILDA, as MATILDA has only a glacier-distributed unit, while mHM is a fully spatially distributed model. In the initial days, MATILDA performance was poor due to the overestimation of the input parameterization. The initial storage condition, glacier area, and elevation distribution are possibly underestimated when Matilda parameterization is performed, which results in some of the ablation period being lost because of the run bias and it is also possible due to less warm-up period. The Olivares basin has only 20% of the Maipo basin glacier with very high altitude and low temperature and provides very low glacier melt to overall glacier melt. Thus, the mHM with MATILDA Olivares

Preprints (www.preprints.org) | NOT PEER-REVIEWED | Posted: 28 June 2023 doi:10.20944/preprints202306.1979.v1

melt model and the mHM without MATILDA Olivares melt models output result doesn't have much difference. To use glacier melt from the MATILDA approach, the mHM melting component is replaced with the MATILDA melt by internalizing it into the mHM model. Model mHM with MATILDA melt performed well in 2015-18 as compared to 2011-15 with having r^2 values of 0.3721 and 0.2532 respectively. Whereas mHM have just 0.2532 and 0.2941. But surprisingly mHM_MAT performed poorly in the initial year of modeling.

To conclude, based on the results obtained, it is indicated that the mHM Model had a good performance to predict runoff and can be a potential monitoring tool for watershed management in a mountainous area. The MATILDA model was able to calculate the impact of glaciers during the summer and autumn seasons but in winter and spring, it performs poorly. The results from both model tools show variations in the results due to spatial resolution differences and their methodology. MATILDA has a glacier retreat routine that gives better result for the glacier characteristics such as 'runoff from the glacier' and 'runoff without glacier' and 'glacier area'. The incorporation of MATILDA melt in a simple approach should be further developed in future research for the whole Maipo catchment, which includes glacier melt distribution in mHM models. The Glacier Modelling approach can be further improved by including solar radiation and Energy balance models, especially for high-altitude glacier regions. Analyzing the sensitivity of the parameters used to calibrate the model.

Table 21. Digital Appendix model folder files details.

		mHM Model	MATILDA Model	mHM MATILDA Model
1.	**Initial Model File:**	mHM Sources (mhm-v5.11.1)Folder Maipo Model (5710001)Folder		mHM Sources (mhm-v5.11.1)Folder Maipo Sub-Basin Model (5710001)Folder
2.	**Input File:**			
	Meteorological Data	Precipitation(pre.nc) Temperature(tavg.nc) Evapotranspi(pet.nc)	Forcing.csv Glacier_profile.csv Runoff_data.csv	Precipitation(pre.nc) Temperature(tavg.nc) Evapotranspi(pet.nc) Mat_melt.csv
	Morphological Data	Aspect.asc Dem.asc Facc.asc Geology_class.asc IDgauge.asc Lc.asc Slope.asc Soil_class.asc	Maipo_basin.shp Maipo_basin.tif Maipo_glacier.shp Maipo_glacier.tif Glacier_thickness.tif	Maipo_basin.shp Maipo_subbasin.shp Maipo_basin.tif Maipo_subbasin.tif Maipo_glacier.shp Maipo_glacier.tif Glacier_thickness.tif
3.	**Preprocessing Files**	Hypsometry.py Resampling melt.py	Input_data_pre.py GIS_routine.py	Input_data_pre.py GIS_routine.py
4.	**Post-processing files**	mHM_Plotting.py	Matilda_Plotting.py	mHM_Mat_Plotting.py
6.	**Final Model Files**	mhm.nml	matilda.py	mhm.nml
	Flies Link	*https://github.com/ahmadmum/msc_thesis_glacier_modelling.git*		

References

1. Ahumada, G.; Bustos, D.; González, M. Effect of climate change on drinking water supply in Santiago de Chile. Sci. Cold Arid Reg. 2013, 5, 27–34.
2. Pritchard, H.D. Asia's shrinking glaciers protect large populations from drought stress. Nature 569, 649–654 (2019). https://doi.org/10.1038/s41586-019-1240-1.
3. Biemans, H. et al. Importance of snow and glacier meltwater for agriculture on the Indo-GangeticPlain. Nat Sustain 2, 594–601 (2019).

4. Barnett, T.P., Adam, J.C., Lettenmaier, D.P., 2005. Potential impacts of a warming climate on water availability in snow-dominated regions. Nature 438, 303–309.
5. Dyurgerov, M.B., Carter, C.L., 2004. Observational evidence of increases in freshwater inflow to the Arctic ocean. Arct. Antarct. Alp. Res. 36 (1), 117–122.
6. Ahmad, M., Al Mehedi, M. A., Yazdan, M. M. S., & Kumar, R. (2022). Development of Machine Learning Flood Model Using Artificial Neural Network (ANN) at Var River. Liquids, 2(3), 147-160.
7. Hugonnet, R., McNabb, R., Berthier, E., Menounos, B., Nuth, C., Girod, L., Farinotti, D., Huss, M., Dussaillant, I., Brun, F., and Kääb, A.: Accelerated global glacier mass loss in the early twenty-first century, Nature, 592, 726–731, https://doi.org/10.1038/s41586-021-03436-z, 2021.
8. Edwards, T. L., Nowicki, S., Marzeion, B., Hock, R., Goelzer, H., Seroussi, H., Jourdain, N. C., Slater, D. A., Turner, F. E., Smith, C. J., McKenna, C. M., Simon, E., Abe-Ouchi, A., Gregory, J. M., Larour, E., Lipscomb, W. H., Payne, A. J., Shepherd, A., Agosta, C., Alexander, P., Albrecht, T., Anderson, B., Asay-Davis, X., Aschwanden, A., Barthel, A., Bliss, A., Calov, R., Chambers, C., Champollion, N., Choi, Y., Cullather, R., Cuzzone, J., Dumas, C., Felikson, D., Fettweis, X., Fujita, K., Galton-Fenzi, B. K., Gladstone, R., Golledge, N. R., Greve, R., Hattermann, T., Hoffman, M. J., Humbert, A., Huss, M., Huybrechts, P., Immerzeel, W., Kleiner, T., Kraaijenbrink, P., Le clec'h, S., Lee, V., Leguy, G. R., Little, C. M., Lowry, D. P., Malles, J.-H., Martin, D. F., Maussion, F., Morlighem, M., O'Neill, J. F., Nias, I., Pattyn, F., Pelle, T., Price, S. F., Quiquet, A., Radic, V., Reese, R., Rounce, D. R., Rückamp, M., Sakai, A., Shafer, C., Schlegel, ´ N.-J., Shannon, S., Smith, R. S., Straneo, F., Sun, S., Tarasov, L., Trusel, L. D., Van Breedam, J., van de Wal, R., van den Broeke, M., Winkelmann, R., Zekollari, H., Zhao, C., Zhang, T., and Zwinger, T.: Projected land ice contributions to twenty-first-century sea level rise, Nature, 593, 74–82, https://doi.org/10.1038/s41586-021-03302-y, 2021.
9. Huss, M. and Hock, R.: Global-scale hydrological response to future glacier mass loss, Nature Climate Change, 8, 135–140, https://doi.org/10.1038/s41558-017-0049-x, 2018.
10. Immerzeel, W.W., Lutz, A.F., Andrade, M. et al. Importance and vulnerability of the world's water towers. Nature 577, 364–369 (2020). https://doi.org/10.1038/s41586-019-1822-y.
11. Cauvy-Fraunié, S. and Dangles, O.: A global synthesis of biodiversity responses to glacier retreat, Nature Ecology & Evolution, 3, 1675– 1685, 2019
12. Rivera, A.; Bown, F.; Acuña, C.; Ordenes, F. I Ghiacciai del Cile come Indicatori dei Cambiamenti Climatici.Chilean Glaciers as Indicators of Climatic Change. Terra Glacialis Edizione Speciale. Special Issue "MountainGlaciers and Climate Changes in the Last Century". 2009. Available online: http://repositorio.uchile.cl/bitstream/handle-/2250/117817/113801_C11_rivera-italia.pdf?sequence=1.
13. Rivera, A.; Acuña, C.; Casassa, G.; Bown, F. Use of remote sensing and field data to estimate the contribution of Chilean glaciers to the sea level rise. Ann. Glaciol. 2002, 34, 367–372.
14. Meza, F.J.; Wilks, D.S.; Gurovich, L.; Bambach, N. Impacts of Climate Change on Irrigated Agriculture in the Maipo Basin, Chile: Reliability of Water Rights and Changes in the Demand for Irrigation. J. Water Resour. Plan. Manag. 2012, 138, 421–430
15. Cai X, Rosegrant MW, Ringler C. 2003. Physical and economic efficiency of water use in the river basin: Implications for efficient water management. Water Resources Research 39(1)
16. Mehedi, M. A. A., Yazdan, M. M. S., Ahad, M. T., Akatu, W., Kumar, R., & Rahman, A. (2022). Quantifying Small-Scale Hyporheic Streamlines and Resident Time under Gravel-Sand Streambed Using a Coupled HEC-RAS and MIN3P Model. Eng, 3(2).
17. Mehedi, M. A. A., Khosravi, M., Yazdan, M. M. S., & Shabanian, H. (2022). Exploring Temporal Dynamics of River Discharge using Univariate Long Short-Term Memory (LSTM) Recurrent Neural Network at East Branch of Delaware River. Hydrology, 9(11), 202.
18. Pellicciotti, F.; Helbing, J.; Rivera, A.; Favier, V.; Corripio, J.; Araos, J.; Sicart, J.-E.; Carenzo, M. A study of the energy balance and melt regime on Juncal Norte Glacier, semi-arid Andes of central Chile, using meltmodels of different complexity. Hydrol. Process. 2008, 22, 3980–3997.

19. Yazdan, M. M. S., Ahad, M. T., Kumar, R., & Mehedi, M. A. A. (2022). Estimating Flooding at River Spree Floodplain Using HEC-RAS Simulation. J, 5(4), 410-426.
20. Yazdan, M. M. S., Khosravia, M., Saki, S., & Al Mehedi, M. A. (2022). Forecasting Energy Consumption Time Series Using Recurrent Neural Network in Tensorflow.
21. Pellicciotti, F.; Burlando, P.; Van Vliet, K. Recent trends in precipitation and streamflow in the AconcaguaRiver Basin, central Chile. In IAHS Assembly; IAHS Publ.: Foz do Iguaçu, Brazil, 2007; pp. 1–22.
22. Masiokas, M.H.; Villalba, R.; Luckman, B.H.; Le Quesne, C.; Aravena, J.C. Snowpack Variations in the Central Andes of Argentina and Chile, 1951–2005: Large-Scale Atmospheric Influences and Implications for Water Resources in the Region. J. Clim. 2006, 19, 6334–6352.
23. Yazdan, M. M. S., Khosravia, M., Saki, S., & Al Mehedi, M. A. (2022). Forecasting Energy Consumption Time Series Using Recurrent Neural Network in Tensorflow.
24. Marzeion, B., Jarosch, A. H., and Hofer, M.: Past and future sealevel change from the surface mass balance of glaciers, The Cryosphere, 6, 1295–1322, https://doi.org/10.5194/tc-6-1295- 2012, 2012b.
25. Abdullah Al Mehedi, M., Reichert, N., & Molkenthin, F. (2020, May). Sensitivity Analysis of Hyporheic Exchange to Small Scale Changes in Gravel-Sand Flumebed Using a Coupled Groundwater-Surface Water Model. In EGU General Assembly Conference Abstracts (p. 20319).
26. Huss, M. and Hock, R.: A new model for global glacier change and sea-level rise, Front. Earth Sci., 3, 1–22, https://doi.org/10.3389/feart.2015.00054, 2015.
27. Khadka D, Mukand S. Babel Sangam S, Nitin K. Tripathi b,2014 Climate change impact on glacier and snow melt and runoff in Tamakoshi basin in the Hindu Kush Himalayan (HKH) region.
28. Mehedi, M. A. A., & Yazdan, M. M. S. (2022). Automated Particle Tracing & Sensitivity Analysis for Residence Time in a Saturated Subsurface Media. Liquids, 2(3), 72-84.
29. Mayr, E., W. Hagg, C. Mayer, and L. Braun (2013). "Calibrating a Spatially Distributed Conceptual Hydrological Model Using Runoff, Annual Mass Balance and Winter Mass Balance". In: Journal of Hydrology 478, pp. 40–49. doi: 10.1016/j.jhydrol. 2012.11.035
30. Mehedi, M. A. A., & Yazdan, M. M. S. (2022). Automated Particle Tracing & Sensitivity Analysis for Residence Time in a Saturated Subsurface Media. Liquids, 2(3), 72-84.
31. Akhtar, M., Ahmad, N., Booij, M.J., 2008. The impact of climate change on the water resources of the Hindukush–Karakorum–Himalaya region under different glacier coverage scenarios. J. Hydrol. 355, 148–163.
32. Hersbach, H, Bell, B, Berrisford, P, et al. The ERA5 global reanalysis. Q J R Meteorol Soc. 2020; 146: 1999– 2049. https://doi.org/10.1002/qj.3803.
33. Pfeffer, W. T., Arendt, A. A., Bliss, A., Bolch, T., Cogley, J. G., Gardner, A. S., Hagen, J.-O., Hock, R., Kaser, G., Kienholz, C., Miles, E. S., Moholdt, G., Mölg, N., Paul, F., Radic, V., Rastner, ´ P., Raup, B. H., Rich, J., and Sharp, M. J.: The Randolph Glacier Inventory: a globally complete inventory of glaciers, J. Glaciol., 60, 537–552, https://doi.org/10.3189/2014JoG13J176, 2014.
34. Jing, M., Heße, F., Kumar, R., Wang, W., Fischer, T., Walther, M., Zink, M., Zech, A., Samaniego, L., Kolditz, O., and Attinger, S.: Improved regional-scale groundwater representation by the coupling of the mesoscale Hydrologic Model (mHM v5.7) to the groundwater model OpenGeoSys (OGS), Geosci. Model Dev., 11, 1989–2007, https://doi.org/10.5194/gmd-11-1989-2018, 2018.
35. Samaniego L., R. Kumar, S. Attinger (2010): Multiscale parameter regionalization of a grid-based hydrologic model at the mesoscale. Water Resour. Res., 46,W05523, doi:10.1029/2008WR007327.
36. Bergström, S. Development and Application of a Conceptual Runoff Model for Scandinavian Catchments. Ph.D. Thesis, Swedish Meteorological and Hydrological Institute, Norrköping, Sweden, 1976.
37. Seguinot, J., Ivy-Ochs, S., Jouvet, G., Huss, M., Funk, M., & Preusser, F., 2018. Modelling last glacial cycleice dynamics in the Alps, The Cryosphere, 12(10), 3265–3285.

38. Reeh ES, Messer HH, Douglas WH. Reduction in tooth stiffness as a result of endodontic and restorative procedures. J Endod. 1989 Nov;15(11):512-6. doi: 10.1016/S0099-2399(89)80191-8. PMID: 2639947.
39. Hock, R., 2003. Temperature index melt modelling in mountain areas. J. Hydrol. 282, 104–115.
40. Seibert, J., Vis, M., Kohn, I., Weiler, M., & Stahl, K. (2018). Technical note: Representing glacier geometry changes in a semi-distributed hydrological model. Hydrology and Earth System Sciences, 22(4), 2211–2224. https://doi.org/10.5194/hess-22-2211-2018.
41. Huss, M., G. Jouvet, D. Farinotti, and A. Bauder (2010). „Future high-mountain hydrology: a new parameterization of glacier retreat “. In: Hydrology and Earth System Sciences 14.5, pp. 815–829. DOI: 10.5194/hess-14-815-2010.
42. Bahr, D. B., Meier, M. F., and Peckham, S. D.: The physical basis of glacier volume-area scaling, J. Geophys. Res.-Sol. Ea., 102, 20355–20362, https://doi.org/10.1029/97JB01696, 1997.
43. Krause, P., D. P. Boyle, and F. Bäse (2005). “Comparison of Different Efficiency Criteria for Hydrological Model Assessment”. In: Advances in Geosciences 5, pp. 89–97.
44. Bergström, H. and Moberg, A.: 2002, ‘Daily Air Temperature and Pressure Series for Uppsala 1722–1998’, Clim. Change, this volume.
45. Nash JE, Sutcliffe JV. 1970. River flow forecasting through conceptual models. Part 1. A discussion of principles. Journal of Hydrology 10(3): 282–290.
46. Kling, H., Fuchs, M. and Paulin, M.: Runoff conditions in the upper Danube basin under an ensemble of climate change scenarios, J. Hydrol., 424-425, 264–277, doi: 10.1016/j.jhydrol.2012.01.011, 2012.
47. Roberts, W., Williams, G., Jackson, E., Nelson, E., Ames, D., 2018. Hydrostats: A Python Package for Characterizing Errors between Observed and Predicted Time Series. Hydrology 5(4) 66, doi:10.3390/hydrology5040066.
48. Refsgaard, JC (1997). Parameterisation, calibration and validation of distributed hydrological models. Journal of Hydrology, 198 (1-4), 69-97. https://doi.org/10.1016/S0022-1694(96)03329-X.